Enhanced Piezoelectric Drop-on-Demand Cell Dispensing through Neutral Buoyancy

by

Daljeet Chahal

B.Sc., The University of Northern British Columbia, 2010

A THESIS SUBMITTED IN PARTIAL FULFILLMENT OF

THE REQUIREMENTS FOR THE DEGREE OF

MASTER OF APPLIED SCIENCE

in

THE FACULTY OF GRADUATE STUDIES

(Biomedical Engineering)

THE UNIVERSITY OF BRITISH COLUMBIA

(Vancouver)

June 2012

Abstract

Micro dispensing of cell based suspensions offers enhanced precision and accuracy for a wide variety of applications including high throughput cell based assays, single cell analyses and tissue engineering. One technology that offers such promises is piezoelectric inkjet printing. However, the small size scale of internal system features makes it difficult to eject particle based suspensions due to undesirable phenomena within the suspension. In particular, it has been hypothesized that inkjet dispensing of cell based suspensions has been hindered by sedimentation and aggregation of cells. The objective of this thesis was to investigate the phenomenon of cellular sedimentation and determine whether it affects piezoelectric dispensing reliability, and to devise a method to mitigate this phenomenon. The challenge in stabilizing suspensions to halt sedimentation lies in constraints involving cellular viability, and the rheological limitations imposed by the capability of the inkjet system itself. We achieved stabilized cellular suspensions through the use of a sucrose co-polymer, Ficoll-PM400. We show herein that stabilizing the suspension to be dispensed through this method greatly improves the reliability of the system over long periods of time, and increases the consistency of cell counts. Cell viability was shown to remain constant even when suspended for periods of 1 hour. The change in viscosity of the suspension also decreased the amount of clogging events that have hampered particle based inkjet dispensing approaches. Lastly, we give recommendations regarding future work on this technology.

Preface

This work was conducted in the laboratories of Dr.'s Karen Cheung and Konrad Walus. The majority of the work has beenaccepted for publication [Chahal D, Ahmadi A, Cheung KC (2012) Improving piezoelectric cell printing accuracy and reliability through neutral buoyancy of suspensions. Biotechnology and Bioengineering, Online publication ahead of print, DOI: 10.1002/bit.24562]. I conducted all of the testing and wrote the majority of the manuscript. Dr. Ali Ahmadi wrote the MatLab script used for sedimentation measurements and provided assistance with technical details. Dr. Ali Ahmadi also created Figures 3.4, 4.4, 4.5, 4.7, 4.8, and 4.9 found in this thesis. Drs. Ali Ahmadi and Karen Cheung edited the manuscript. All three authors helped to design experiments.

Table of Contents

List of Tables

List of Figures

Acknowledgements

I would like to thank Dr. Karen Cheung for her support and encouragement over the last two years. Her ability to analyze problems and instantly come up with creative solutions never fails to impress me. The time spent in her research group has exposed me to subject areas and research problems I would have never otherwise knew existed. It has been both very gratifying and humbling working with talented individuals of different technical backgrounds. I believe the skills and knowledge I have gathered here will be invaluable for my future career aspirations.

I would like to extend my appreciation to Dr. Konrad Walus, who has graciously provided resources for my tenure here. I would like to also thank him and Dr. Boris Stoeber for serving on my thesis committee. I would also like to greatly thank Dr.'s Ali Ahmadi and Linfen Yu, who have provided me with great one-on-one guidance for as long as I have known them. I would like to thank members of the lab whom I have provided both support and great comedy over the years. Jonas, Sam, Nomin, Kevin, Chris, Fabienne, Simon, and anyone my failing memory has forgotten. I appreciated all the fruitful discussions.

Lastly, I would like to thank my parents, Avtar and Manpreet Chahal. Thank you.

Chapter 1: Introduction

Small volume liquid handling techniques for life science applications have garnered significant interest over the last 20 years. The field has evolved from the exclusive use milliliter scale tools such as Pasteur pipettes to the large scale and high throughput adoption of microliter scale technologies such as automated robotic systems and multi-well plate technologies. Technologies such as microfluidics have pushed the envelope on small volume handling even further, opening up the possibility of assaying large quantities of biological events in parallel with minimal reagent use. Additionally, the combination of small volume fluid handling and precise positional control open up possibilities for precise high content cell biology screens for drug screening applications, single cell analysis, and the exploration of tissue microarchitecture based on cell position for applications in tissue engineering. This combination of small volume fluid handling and positional control already exists in a technology that has become ubiquitous in the world, inkjet printing.

Inkjet printing has its roots with the nineteenth century physicist, Lord Kelvin, who originally dreamed of guiding droplets through an electrostatic field. He could not deliver on his vision, however, due to a lack of experimental resources. The first commercial applications of inkjet printing were pioneered in the 1950s by Siemens, which was followed by massive development in the following decades. Today, inkjet printing has become ubiquitous through the world of desktop publishing, a testament to its usability. The term inkjet printing actually encompasses a range of technologies; a particular subset known as piezoelectric drop-on-demand printing has become a popular choice for industrial applications.

All inkjet technologies accomplish the same fundamental tasks, albeit through different physical mechanism. These tasks can be separated into three distinct phases. The first involves the generation of a droplet at the liquid air interface of the inkjet nozzle's orifice. A pressure wave is created within the fluid, which propagates towards the interface. A droplet will emerge if this wave transfers more kinetic energy outwards than the surface energy that is needed to form a drop. In the case of piezoelectric drop-on-demand printing, this wave is created by direct actuation of a piezoelectric element, and is done so only when ejection of droplets is needed. The second phase involves the immediate interaction of the droplet with the substrate. The speed of the droplet and the physical properties of the liquid and substrate will dictate the extent of spreading upon impact, which has significant bearing on final feature morphologies. Lastly, the manner in which the deposited droplet evaporates will have an impact on the distribution of the deposited solute residue. Indeed, the "coffee ring" effect which plagues many printing efforts is a direct result of evaporation phenomena.

Although the previously described phenomena are well known, they have all been characterized using Newtonian fluids; in fact, inkjet printing has always been intended for use with low viscosity and well dispersed Newtonian fluids. However, research into the use of inkjet printing for experimental fluids has become widespread. Many of these experimental fluids display non-Newtonian behaviours. A major challenge of applying inkjet printing for the dispensing of such experimental fluids is to account for these behaviours and then devise methods to mitigate them. In biology, the fluid to be dispensed is often a suspension of cells. Cells are large enough that they experience many physical forces over the course of dispensing; this may alter their distribution within the fluid. Furthermore, biological interactions between surface proteins will lead to the aggregation of these cells,

another factor which may confound inkjet performance. In addition, one must take into account that biological applications require appropriate environmental conditions in order to ensure effective post printing viability and utilization. Herein lies the challenge of applying inkjet technologies for biological applications; a formulation for the biological "ink" must be devised, which both optimizes inkjet performance and preserves the integrity of the cells.

This thesis presents a method that prevents the sedimentation and associated aggregation of cells during inkjet printing. A simple addition of a sucrose co-polymer to the cellular suspension ensures density matching between the cells and the surrounding media. It was found that the addition of polymer to the suspension mitigated cell sedimentation, ensured appropriate cellular dispersion, and remained within the viscosity range permitted by inkjet printing. This addition of polymer was found to greatly increase the accuracy and reliability of cell based piezoelectric drop-on-demand printing. Lastly, a decrease in nozzle clogging was also observed, and this phenomenon was characterized. This thesis consists of the following five chapters:

- Chapter 1: This chapter provides an introduction to micro scale fluid handling technologies and inkjet printing, as well as how such technologies are gaining rapid ground in the biological sciences. Applications, competing technologies, and associated technical challenges are presented.
- Chapter 2: This chapter presents a detailed theoretical background associated with inkjet printing and particle suspensions. The physical process and mechanism of inkjet printing is presented and detailed. The physical and biological processes present within a suspension of cells are also presented, and details are given as to how these processes would interfere with the inkjet printing process.

- Chapter 3: This chapter presents the rationale and method taken to achieve a neutrally buoyant suspension ready for piezoelectric dispensing. Constraints dictated both by cellular components and the piezoelectric system are highlighted. The specifics of the compounds utilized in our approach are also presented.
- Chapter 4: This chapter presents an analysis of the observed experimental results. Various observations and resulting phenomena are highlighted. Suspensions are formulated, characterized, and tested for cell compatibility. Improvements to the inkjet printing process are demonstrated. A thorough discussion of the results and observed phenomena is given.
- Chapter 5: This chapter summarizes the experiments and findings of the thesis and highlights the remaining challenges. Recommendations regarding the next steps of relevant research topics are given.

1.1 The Growth of Micro Scale Liquid Handling Technologies for Cell Biology Applications

The biological and chemical sciences depend fundamentally on the handling and transfer of solutions and suspensions. The field of liquid handling technology has evolved greatly over the past 20 years [1] . Technology has adapted from large, manual pipette tools to automated and miniaturized robotic systems capable of dispensing fluids into multi well plates. High throughput systems have also greatly benefited from the development of appropriate assay techniques. The number of individual samples on multi well plates has increased, with 1536 wells on a single plate now being routine. However, a bottle neck has been reached for high throughput systems. Further progression is now limited by the

development of further liquid handling technologies. The advent of microfluidic technologies are now beginning to fill this gap, and have led to breakthroughs in areas such as protein crystallography [2]. Other micro dispensing technologies, such as inkjet printing, have also been gaining popularity among those in the drug screening and tissue engineering fields. The potential for accurate and high-throughput cell handling techniques solves many problems and opens up many opportunities for both of these fields. Herein, we discuss some of these possibilities.

1.1.1 High Content Screening, Pharmaceutical Applications

High content screens in the biotechnological and pharmaceutical industries have become widespread. These screens involve the plating of cells, treatment with particular compounds of interest, and assessment through various assay methodologies. One of the largest problems associated with such cell based screens is the introduction of false positives and false negatives [3]. Such false results can have massive impact on downstream assessment of drug compounds; errors can lead to large financial costs. These errors are often due to mismatched numbers of cells being dispensed from well to well, which occurs due to the low accuracy of robotic liquid handling techniques implemented in such settings. Read out assays are very sensitive to the number of cells being tested, and yet no accurate high-throughput method for controlling the number of cells within these assays is implemented. Furthermore, this effect is compounded to the low statistical rigor of the entire drug screening workflow. Very large numbers of compounds are tested for their potential effects on such cells in primary screens, however, only a single measurement of each compound's activity is obtained during this phase [4]. This is generally due to the cost of reagents; more tests are simply not feasible

given budgetary restraints. This can lead to measurement errors, for example, compounds with highest measured activities during primary screens will yield less activity during secondary screens due to a statistical artifact known as “regression toward the mean” [5]. Likewise, positive hits from the primary screen which yielded low activity levels may not show any activity at all during secondary screens. Multiple measurements are known to reduce such artifacts.

Small volume liquid handling systems such as inkjet printing could overcome these barriers and also open up new possibilities in the high throughput drug discovery arena. The on demand generation of picoliter volume droplets serves as a method to accurately control dispensed volume. These smaller volumes could accommodate multi well plates of increasing content, and save on reagent costs. Statistically relevant metrics, such as assessment of compound activity variances and random error, could be incorporated into screens due to increased measurement capabilities. Also, such handling techniques are leading to the creation of “cell microarrays”, in a vein similar to the DNA microarrays that have gained widespread adoption [6]. These arrays will serve to reduce the complexity of high content screens, by increasing parallelization and decreasing technical complications involved with reagent and cell removal from multi well plates. More significantly, such small volume cell handling techniques, combined with appropriate assays, could enable high throughput and large scale interrogation of cellular networking systems in a systems biology approach. This refers to assessing the effects of drug compounds on various molecular aspects within a cell simultaneously instead of focusing on one particular molecular target one at a time [7, 8]. Such screens will ultimately be needed if the inefficient preclinical development pipeline is ever to improve its reliability.

1.1.2 Positional Significance, Tissue Micro Architecture and Microenvironment, Tissue Engineering Applications

The geometrical and physical makeup of a tissue is becoming an ever increasing topic of interest in the biological sciences [9]. This interest originally emerged after application of physical forces to cells was shown to impact genetic expression and phenotype. An example includes the generation of rotational shear stress to cellular receptors through the binding of antibody coated magnetic microspheres; the magnitude of rotation was shown to influence the behaviour of the cells due to reshaping of the internal cellular skeleton [10]. The field of tissue engineering has spurred from efforts to create tissue mimics. The field has also extended from the goal of creating replacement tissues to using such mimics for basic research as well as identification of novel drug compounds [11].

The importance of the precise positioning of cells within cell cultures is now accepted. Investigations of the influence of cell position on cell growth, migration and division have been conducted. The influence of cell position on tissue generation is also now being carried out [12]. Additionally, the idea that the environment surrounding the cell, known as the “cellular microenvironment”, plays a large role in cellular processes has also gained traction among the biological community. We can summarize the concept of the microenvironment by saying that the overall phenotypical response of a particular tissue is a function of the cell types it consists of, the interactions of these cells with one another, the interactions of these cells with the surrounding tissue matrix (fiber network of proteins), and the presence of various soluble factors. Comprehensive review of this matter can be found elsewhere [13]. Although there is an agreed understanding that micro architecture is critical

to the function of tissues, the field remains wide open for exploration. A key issue with this is that the tools commonly used to probe tissue micro architecture are slow and cumbersome, even if very precise. These tools are those of micro fabrication, which will be discussed later. Furthermore these tools do not allow on demand customized positioning. Inkjet printing could serve as a means to rapidly explore positional parameters in such settings.

Lastly, large scale industrial generation of cell based micro tissues (for example, manufacture of biological implants or micro tissues in a drug screening setting) will depend on the ability to reliably place cells in desired locations with high confidence of repeatability. Inkjet printing again may provide the ideal solution for this situation.

1.2 Cell Patterning Technologies – State of the Art

Cellular micro patterning is a field that has achieved large growth over the last decade due to the realization that tissue microarchitecture influences function. This field heavily depends on the development of technologies that can precisely manipulate cell position. These technologies can be classified into two groups, indirect patterning or direct write methods. Indirect methods are those that utilize environmental factors, such as geometry and fluid flow, to direct and confine cells to desired locations. The processes of microfabrication and soft lithography are utilized to create patterned substrates and devices that can be used to create defined cell cultures. Indirect patterning methods have gained significant adoption in the scientific community, and are hence worthy of a brief review. Direct write methods are those that involve the deposition of cells to arbitrary areas, and are therefore not dependent on particular aspects, such as surface features, of the substrate (although substrate modifications may be needed to ensure cellular attachment). Various technologies

encompassed in these groups are discussed herein. Basic processes are described, examples of technological utilization relevant to drug screening or tissue engineering fields are given, and both advantages and disadvantages are discussed.

1.2.1 Microfabrication and Soft Lithography Based Methods

Microfabrication refers to the manufacture of micrometer or smaller size scale structures. A combination of technological approaches, including photolithography, doping, thin film deposition, etching and bonding, are used subsequently to fabricate devices. Many devices involve a large number of fabrication steps, complicating processes. Photo masks are generally used to etch patterns into substrates such as silicon. Microfabrication is a vast field; comprehensive reviews on both techniques and applications relevant to fields of interest can be found elsewhere [14, 15].

Soft lithography is a process where a polymeric material is used for rapid prototyping of devices [16]. The process is cheap and simple, making it ideal for large scale device testing. A silicon master pattern is made using microfabrication. Polydimethylsiloxane (PDMS) is an elastic polymer which is used to create a mould of the silicon master. A second master can then be created from this PDMS mould by using a material such as polyurethane. By using this polyurethane master, PDMS replicates can then be created in large numbers. This eliminates the need to re-fabricate patterns in the cleanroom for each desired experiment.

Although a single pattern can be tested numerous times with this process, cleanroom fabrication is still required every time a new pattern is to be created. As such this limits the rate at which geometrical parameters can be explored. However, the precise structures that

can be created using these approaches is impressive; single cells can be manipulated as desired [17]. Some methods involving the soft lithographic approach are presented.

Confinement

Perhaps the simplest application of soft lithography in the realm of cellular micro patterning is the approach of confinement. An array of spatially separated chambers is created in PDMS. These chambers are then placed in the culture substrate. For example, a circular PDMS mould containing a predetermined number of through holes could be generated and then placed into a cell culture dish. Cells could be cultured within these chambers, and once attached, the chamber could be removed. At this point, a second type of cell could be cultured alongside the first to create a two cell type co-culture, or the growth of the cells could be monitored. Such a mould is referred to as a PDMS "stencil". Also, rather than directly culturing the cells within the stencil, the chambersmay be used to incubate protein solutions which adsorb to the surface. Seeded cells may then be preferentially attached to these protein islands. Preferential surface attachment, as well as other patterning techniques, is shown in Figure 1.1.

A striking example is the use of such stencils to explore how the culture environment between hepatocytes and fibroblasts impacts hepatocyte function [18]. Stencil patterns were used to create collagen islands to which hepatocytes attached. Fibroblasts were cultured around the hepatocyte islands. Island size, and center to center spacing between islands were varied, and hepatocyte function was assessed based on the release of physiologically relevant chemical species. Furthermore, these cultures were assessed for their ability to predict toxicological drug response as measured by metabolic activity assays. It was found that such

patterned co-cultures were much better at predicting drug response, and that the biological behaviour of these cultures, assessed through albumin and urea production as well as genetic profiling, was much more correlated with physiological behaviour when compared to monolayer hepatocyte cultures.

Micro-Contact Printing

Micro-contact printing is another method based on soft lithography which exploits the creation of micron size features for the patterning of proteins, which directs cell attachment. Elastomeric pillars in the desired arrangement are created through the combination of microfabrication and soft lithography, which are then submerged in a solution of choice [19]. The solution is simply "stamped" onto the desired substrate. Micro-contact printing differs from the patterns possible through confinement techniques due to the size range of patterns; a single cell can be interrogated for its attachment response to particular patterns. Customization of the physical manner in which protein ligands are presented to cells is the key advantage of this approach. Such control of substrate properties is important to many areas of tissue engineering and could lead to a more accurate means of controlling cellular behaviour.

Microfluidic Patterning

A last application of microfabrication to cellular patterning is through microfluidics. The creation of microfluidic devices for cellular patterning can be accomplished by the flow of cells into desired chambers [20]. Such techniques can also be combined with polymer and gel materials, such as matrigel, which is a gelatinous protein mixture mimicking the

extracellular environment [21]. An impressive demonstration of such patterning was shown where a microfluidic device was used to create multi-component cell laden hydrogels. That is, multiple types of hydrogels were used, and the nucleation of one fiber network from another was exploited, creating a continuous polymer network that transitioned from one polymer type to another while providing housing for cells [22]. Specifically, collagen gel precursor surrounded in alginate solution was flowed through a microfluidic channel and then gelled by raising temperature. The alginate was then also gelled through addition of calcium ions. A second collagen doped solution (consisting of fibrinogen instead of alginate) was flowed through an adjacent channel and gelled in the same manner. The collagen network from the first gel continued seamlessly into the second gel. This patterning was also demonstrated when cells were present in the solutions. Microfluidic patterning takes advantages of phenomena including laminar flow and shear forces to direct cells to desired locations.

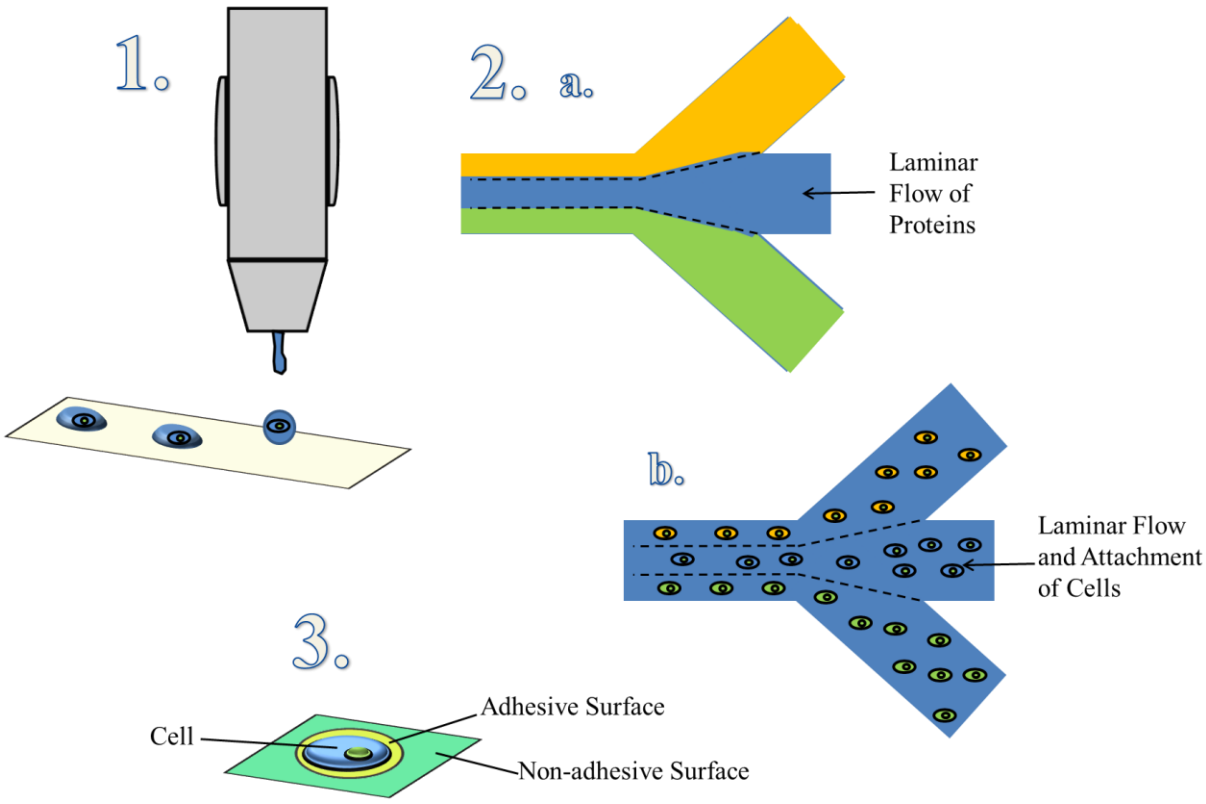

Figure 1.1. Examples of different cellular micro patterning techniques. 1. Direct write techniques, such as inkjet printing, can be used to place droplets containing cells at arbitrary locations. 2. Microfluidic devices can be used to pattern cells through laminar flow by first flowing attachment proteins through channels (a), and subsequently flowing cells through the channels (b). Cells will attach to specific proteins adsorbed to the channel. 3. Deposition of adhesive compounds to substrate through either direct deposition or confinement chamber can be used for preferential attachment of cells to these points.

1.2.2 Direct Write Techniques

Although microfabrication techniques are a powerful means of patterning with very high resolution, they may require significant upfront capital and the generation of new masks for each unique pattern. Furthermore, such facilities may be inaccessible for many scientists. The make-up of biological tissue is complex; how different design parameters influence phenotypical behaviour will need systematic characterization.

As an alternative to lithographic based approaches for cell patterning, many direct write methods have emerged. These technologies do not require the creation of a photo mask and subsequent fabrication within a cleanroom setting. They allow for rapid and custom creation of specified patterns, and may overcome difficulties associated with microfabrication techniques. A brief sampling of direct write methods is given here.

Dip – Pen Nanolithography

The most technically challenging direct-write method, dip-pen nanolithography utilizes atomic force microscopy principles for the creation of patterns at the nano scale [23]. The same stage and cantilever set up used for imaging within atomic force microscopy is adapted by dipping the cantilever in the material to be patterned, which is then used to draw the pattern of choice. This technique has been utilized for DNA and protein patterning. Indeed, extremely high density protein based arrays can be created using this technology [24]. The technique has also been used to precisely generate patterns for cellular attachment [25]. As precise as this technique may be, it likely will not gain dominance as the technology of choice for tissue engineering applications (at this stage in development). The lack of high through-put capabilities will be the first deterrent. Secondly, although manipulation of one cell at a time may provide impressive insight into biological phenomena, it is simply not a practical means of creating a large number of micro tissues at once. Lastly, dip-pen nanolithography is a contact based approach; direct contact with the substrate may introduce unwanted contaminants when dealing with biologically sensitive cells. Nonetheless, a technology of this sensitivity and precision will likely gain ground in many biological applications over time.

Extrusion Based Systems

Many tissue engineering applications require the generation of structures of relatively large size scale and physical integrity. In particular, tissue scaffolds are on the size scale of millimeters or greater, and must be designed to withstand the physical stresses they will incur as an implanted structure [26]. Although micron scale resolution is desirable, micron scale patterning systems do not yet display the throughput required for practical generation of such scaffolds. Also, they are not capable of dispensing the rather viscous materials needed for such scaffolds.

Extrusion based systems capable of producing three dimensional structures have recently been used for these tasks. Such structures have been used to study basic cell biology [27, 28]. Hydrogel and polymer suspensions containing cells have also been dispensed using such systems [29]. Spheroids and cell based "slurries" have also been dispensed, and very interesting post deposition behaviour has been demonstrated [30]. For example, the placement of spheroids in a circular geometry, under appropriate perfusion conditions, resulted in the merging of the separate spheroids into a single structure. Tissue engineered scaffolds are now being tested in animals [31], and extrusion based systems may be the best means to produce these on a large scale.

These systems depend heavily on the particular materials that are used. Further progress in this field relevant to biological and medical applications will depend on the ability to generate materials that provide superior patterning control while preserving cellular function. Currently, such materials are lacking, and limit the resolution and cell type specific applications possible [32].

Droplet Based Techniques

A rather intriguing recent innovation has been the use of laser printing for the deposition of cells [33]. A variety of cell types have been deposited using such a technique, and varying levels of post printing cell viability have been demonstrated.

Laser assisted bioprinting (LAB) involves the use of a pulsed laser source, a layer that is coated with the material to be printed, and a receiving substrate [34]. Briefly, a thin source film, which is the cell suspension, is spread onto an optically transparent quartz material. This film is in close contact to the receiving substrate, and the generation of a laser pulse will transfer film material to the substrate. The volume of the deposited material depends linearly on laser pulse energy, and a minimum amount of this energy must be generated in order to overcome surface tension thresholds. LAB presents the advantage of higher frequency printing when compared to methods like inkjet.

Novel printing methods have also been demonstrated. An example is the generation of droplets from an open pool of liquid by the focusing of acoustic waves [35]. The technique has been used to eject and deposit droplets of cells, and comprehensive statistical characterization has been carried out. The lack of a nozzle may overcome deposition and clogging issues associated with other techniques. However, this work also showed that the number of cells dispensed per drop were higher than expected at increased cell concentrations. The authors proposed that the presence of acoustic waves at the focal point causes cells to circulate and accumulate at this point, particularly at higher concentrations, which then results in a higher number of cells being ejected per droplet than expected.

However, we believe that his phenomenon may also have to do with cellular sedimentation, an issue that is tackled in this thesis.

Inkjet Printing for Cell Biology

A technique that has gained significant traction in recent times is the method of inkjet printing. The first demonstration of this concept of placing cells in particular locations via a printer was accomplished by Robert Klebe, and referred to as "cytoscribing" [36]. Thomas Boland and co-workers have popularized this concept in recent times by demonstrating the use of a thermal inkjet printer for deposition of both cells and proteins that induce cellular attachment [37, 38]. Due to inkjet's widespread use for prior applications, the technology is relatively easy to access for experimental use. In contrast to other discussed technologies, cell patterning through inkjet printing could therefore be rapidly adopted by the scientific community. The concept of inkjet bioprinting is already being explored by many academic groups. In addition to Thomas Boland's work, other notable efforts include those by Brian Derby's group at the University of Manchester [39] and by Anthony Atala's group at the Wake Forest Institute for Regenerative Medicine [40].

Inkjet printing encompasses two main technologies, thermal and piezoelectric, with the main concept being the generation of a picoliter volume droplet through creation of a pressure wave. There are a number of publications exploring the technology for use in biomedical applications. In fact, inkjet printing is already widely used for the generation of DNA microarrays [41], highlighting its potential to provide a sterile and biocompatible environment. Furthermore, there has been much interest in its small volume dispensing capabilities to improve work flow procedures in pre-clinical drug development labs [42].

There have been a number of publications exploring the use of the technique for cellular dispensing and patterning [43, 44]. Lastly, direct printing of cells into wounds has even been demonstrated as an attempt to have "on the spot" cellular therapy [45].

Cell viability has been shown to remain high after printing for many different cell types [43, 46]. Furthermore, particular printing parameters such as cell concentration, voltage amplitude, and pulse length have been characterized extensively for their effect on viability [47, 48]. The types of cells that have been patterned are wide ranged, including Chinese hamster ovary (CHO) cells [47], neural cells [43], muscle cells [49], various types of stem cells [50] and bacterial cells [51]. The technology has been used to create various patterns and explore multi cellular interactions [52], as well as create capsules containing cells intended for implantation [53]. Physical aspects of the technology have even been exploited to transfect cells while they are being dispensed [40]. Parallel arrays of nozzles dispensing cells have been explored for their capability in high content screening [54]. Lastly, three dimensional structures embedded with cells have been created by exploiting polymerization reactions such as calcium alginate solidification [55]. It should be noted that various cell attachment proteins and growth factors have been patterned using inkjet printing to influence how cells cultured on top of these patterns will behave [56].

Molecules such as DNA do not pose many problems for the dispensing process because they are not of sufficient size; the impact of shear and gravitational forces can effectively be negated. However, cells do not fall into this size regime and the influence of forces such as gravity, shear, and inertia can be significant. This creates technical challenges with dispensing that must be overcome prior to wide scale use. Such challenges include sedimentation and aggregation of cells, which can lead to uneven distribution of cells over

the volume of the fluid, as well as the deposition and subsequent formation of cell clusters at various locations throughout the inkjet system. Such difficulties have been alluded to in previous work. Saunders and associates showed the cell counts did not remain consistent over an extended printing period, possibly due to sedimentation [46]. This observation was also made when attempting to adapt systems for high content cell-based screening applications [57]. Clogging of the nozzle orifice has also become a common problem when attempting to print cell based suspensions [58]. These problems will have to be overcome for wide spread cell based application of this technology. However, problems such as sedimentation, aggregation, and clogging due to cells within inkjet systems have not yet been characterized extensively [59]. Concrete solutions to such problems do not exist. We have attempted to address some of these challenges through changes in solution density. Within this work we propose a rheological method for achieving neutral buoyancy in solution, characterize the impact of the resulting suspensions on cellular viability, assess their compatibility with piezoelectric inkjet printing, and determine whether the process of achieving neutral buoyancy within cellular suspensions yields improvements in inkjet printing accuracy and reliability over time.

Chapter 2: Rheological Properties

The investigation of the potential scale up of inkjet printing for cellular dispensing involves two important processes. The first is the creation of a stabilized cellular suspension that meets the physical limitations imposed by an inkjet system. The second is the actual assessment of inkjet performance over an extended period of time when using the stabilized suspensions. This chapter will present a detailed explanation of the inkjet process, the phenomena which can affect its performance when dispensing cell based suspensions, and the rationale behind the means taken to improve this performance.

First, the basics of inkjet printing are presented. The physical principles of the system are introduced in order to present the limitations which must be imposed on fluids that are to be dispensed. Second, the fundamentals of particle behaviour within suspensions and how such behaviour pertains to inkjet performance are explained. This behaviour encompasses many physical processes such as sedimentation, aggregation and deposition, and may impact inkjet performance through means of disturbed dispersion or alteration of nozzle performance. Third, the means of creating a cellular suspension formulation to improve performance is detailed. Specifically, limiting concerns such as cellular viability and neutral buoyancy are discussed and the rationale for the use of the sucrose polymer, Ficoll-PM400, is given. A theoretical model accounting for sedimentation of cellular aggregates is also presented.

2.1 Inkjet Printing

The term “inkjet printing” describes several related technologies, all of which use physical force to eject very small volume droplets at precise locations [60]. These technologies include continuous and drop-on-demand systems. Both methods are capable of generating small droplets, whose diameters fall in the range of 10 to 150 μm.

2.1.1 The Various Inkjet Technologies

There are two fundamental inkjet technologies, continuous and drop-on-demand. In continuous inkjet printing, a stream of liquid is formed, but quickly becomes unstable. This is a phenomenon known as Rayleigh instability. This break-up of the liquid stream results in the formation of individual droplets, which are then deflected to precise locations using an electric field. Collection gutters are used to gather droplets that are not deflected correctly. Droplets collected within these gutters are recycled, resulting in economic usage of ink. However, this recycling process may also introduce contaminants into the fluid, a concern that is of high importance in biological applications. As such, continuous inkjet printing was not utilized in this work, and will not likely find acceptance for biological applications [61].

In drop-on-demand inkjet printing, drops are only ejected when they are needed. A pressure wave is generated which travels through the liquid medium. If the force propagated by the wave is above a critical threshold value, it will overcome the surface tension that is present at the fluid-air interface of the nozzle orifice. A finger like projection of the liquid will emerge from the orifice; a droplet will pinch off and continue to project downwards, while the remaining fluid will retract back into the nozzle chamber. Fluid properties will impact how quickly a pressure wave can travel, and the force needed to overcome surface

tension at the orifice. A back pressure is usually applied to keep fluid within the nozzle chamber, which also contributes to the pressure needed to generate a droplet. Drops in these systems are generated using acoustic frequencies (1 – 20 kHz), and as such, acoustic resonance within these systems can strongly influence the propagation of the pressure wave and subsequent droplet formation [62].

Drop-on-demand technologies come in two forms, thermal and piezoelectric, as depicted in Figure 2.1. Thermal technologies utilize a small thin-film heater inside the fluid chamber which can be used to increase the temperature of fluid in the immediate vicinity above its boiling point. A bubble is created, and once heating is stopped, the bubble will collapse. This rapid expansion and collapse will generate a pressure wave. In piezoelectric systems, a piezoelectric transducer is used to create direct mechanical actuation of the nozzle chamber. This actuation generates the required pulse. Piezoelectric technologies allow for control of the length of the actuation pulse, which can be important for droplet formation. In this thesis, a piezoelectric drop-on-demand system (MicroDrop Technologies GmBH) with an 80 μm diameter nozzle (MicroFab Technologies Inc.) was used for all experiments.

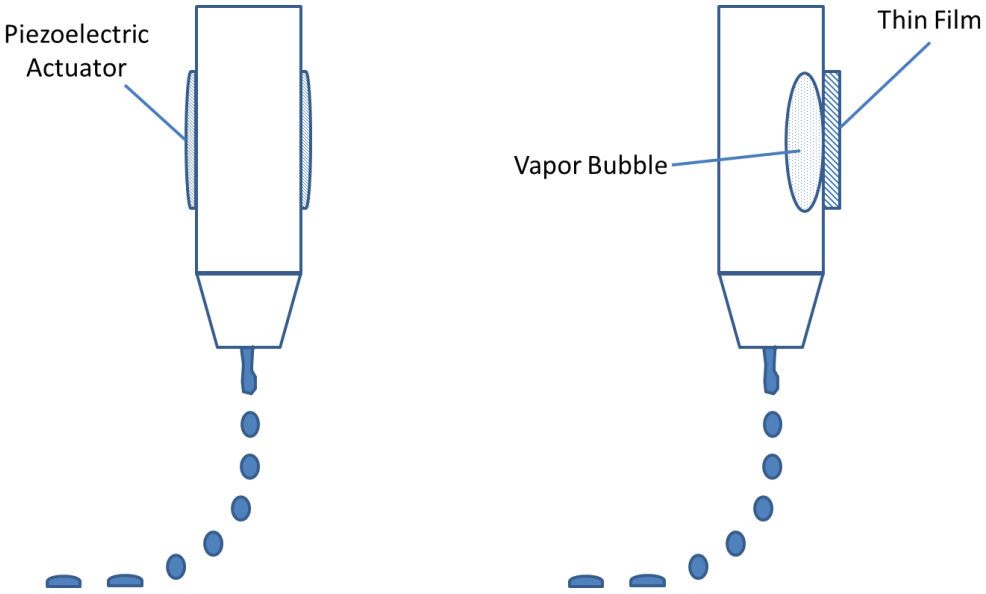

Figure 2.1. Schematic of piezoelectric (left) and thermal (right) inkjet technologies. Piezoelectric actuators can be used to deliver direct mechanical pulses to the nozzle creating waves within the fluid chamber. Thermal technologies utilize a thin film heater to create a vapor bubble that that generates a pressure wave.

2.1.2 Pressure Wave Generation and Acoustic Behaviour

As has been said, the ability of a droplet to form depends on whether the kinetic energy created by actuation is great enough to overcome the surface energy at the liquid air interface [63]. This depends heavily on rheological properties, as will be discussed in section 2.1.3., but the fundamental operation by which droplet formation is accomplished is through the generation of an appropriate pressure wave. The wave generation process, associated dynamics, and influencing parameters will be outlined here in a piezoelectric drop-on-demand system will be discussed here. It should be noted that multiple type of piezoelectric actuated nozzles with varied geometries exist; in this work we have utilized a "squeeze-mode" nozzle type. This type of nozzle consists of a glass capillary with a piezoelectric transducer wrapped around the capillary at the mid-point. Additionally, application of

voltage to the piezoelectric transducer is accomplished through a wave form. Wave forms can be either unipolar or bipolar. Bipolar pulses can be useful for slowing the oscillation of the meniscus after drop ejection [64]. In this work, a unipolar pulse was utilized.

In the squeeze mode inkjet nozzle, a voltage pulse will cause radial displacement of the tube, and whether the radius increases or decreases depends on the polarization of the piezoelectric element. In the MicroFab nozzle, a positive voltage pulse causes fluid expansion. This creates a negative pressure wave which travels in two directions; one wave travels towards the inlet while the other travels towards the orifice. Because the nozzle orifice is small compared to the cross-sectional area of the capillary, it can be considered a closed end [65]. The inlet however, is considered an open end because of the large diameter of the inlet tube relative to the capillary. Due to this, a wave that is reflected from the open end will have its phase shifted by 180^0, whereas the wave reflected from the closed end will maintain its phase. As the waves travel back to meet in the middle of the capillary, voltage drops and the actuator will move radially inward. A unipolar pulse results in contraction back to the original position, whereas a bipolar pulse would contract the nozzle further. Contraction of the nozzle causes a new positive pressure wave to be created at the same moment when the reflected waves meet. The interaction of all of these waves results in negation of the negative waves and doubling of the positive wave [66]. This positive wave then moves toward to orifice, and if it possesses sufficient kinetic energy to overcome the encountered surface tension, a droplet will emerge from the nozzle. This process is depicted in Figure 2.2.

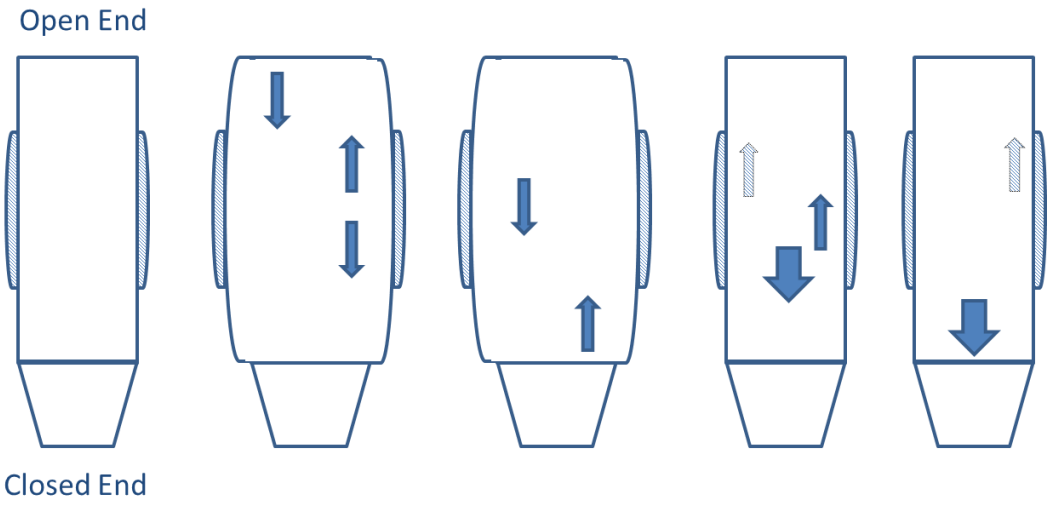

Figure 2.2. Representation of the acoustic phenomena that takes place during nozzle actuation when using a unipolar pulse. The orifice of the nozzle is relatively small compared to the cross sectional area, and can be effectively modeled as a closed end. Outward expansion of the nozzle will cause a wave to be generated that travels in both directions. The wave traveling toward the open end has its phase reverse, whereas the other does not. The waves meet at the center as the nozzle contracts, resulting in the creation of a double positive wave heading towards the orifice. The returning waves degenerate.

2.1.3 System Parameters Influencing Wave Generation and Propagation

One of the great advantages of piezoelectric inkjet systems is the ease of parameter customization. In particular, applied voltage, wave form shape, and frequency of operation are all easily manipulated. Wave generation, and subsequent droplet formation, are inherently dependent on these parameters. Physical properties, such as length of the nozzle capillary, also influence wave propagation.

As mentioned, applying voltage to the piezoelectric transducer is accomplished through a wave form. The shape of the wave form can be changed manually; the different steps correspond to the expansion and contraction of the nozzle outlined in the previous section. A sample unipolar wave form is shown in Figure 2.3. Both the amplitude (magnitude

of voltage) and pulse length (overall time taken for wave form) influence the drop formation process. Increases in amplitude lead to larger transducer displacement, larger volume displacement, and correspondingly larger pressure waves and fluid acceleration. Increasing amplitude increases both droplet volume and velocity in a linear manner, within a limited range. This range is found between the minimum voltage amplitude needed for drop ejection and the voltage limit which causes maximum displacement of the piezoelectric element. However, pulse length evokes a more complicated relationship with droplet behaviour [62]. In particular, droplet velocity has been shown to exhibit a maximum as a function of pulse width. This maximum remains unchanged when driving voltage amplitude is increased, but shifts when fluid properties are changed.

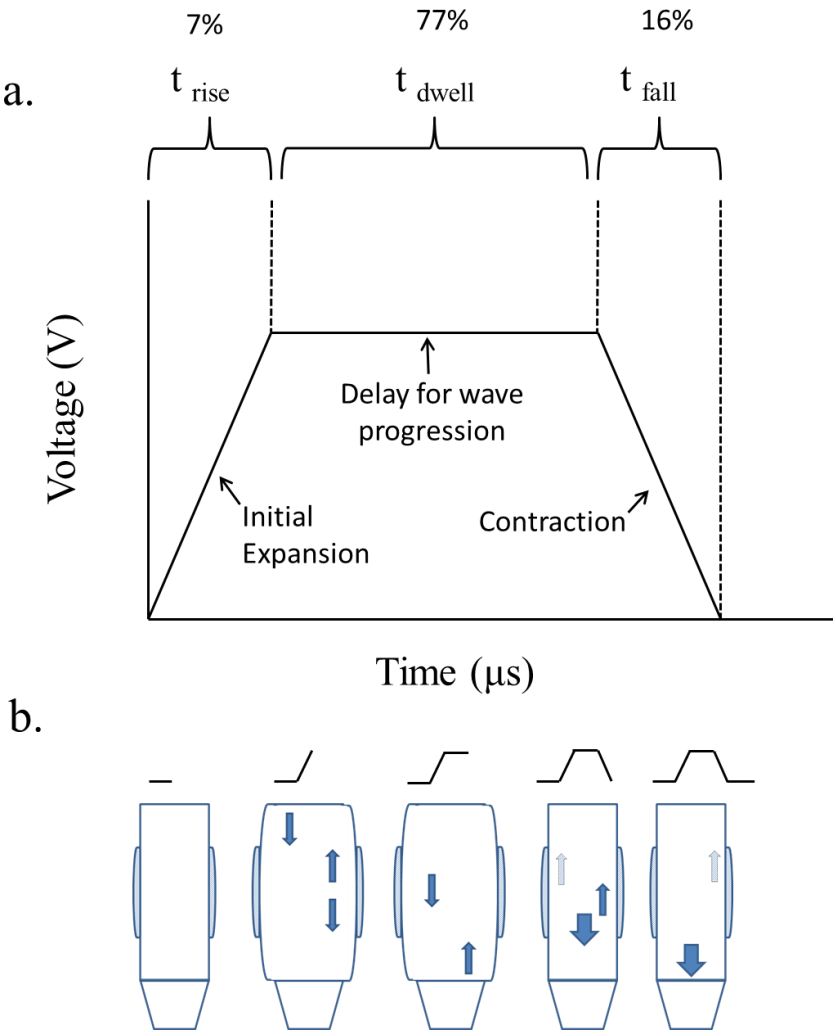

Figure 2.3. Depiction of a typical unipolar wave form used for piezoelectric dispensing. **A**. This is a one sided wave form (positive voltage), consisting of a rise time, dwell time, and fall time. The inkjet system used in this study (Microdrop Technologies GmbH) utilizes this type of wave form. The percentages indicate the relative contribution of the rise, dwell, and fall times to the pulse length. Pulse lengths in this study ranged from 16 to 23 µs. **B.** The relation of wave form progression to the process of wave generation within the nozzle.

Frequency of piezoelectric element actuation is also fundamentally important to acoustic phenomena [66]. High frequency results in chaotic drop formation, as the earlier pressure waves have not yet completely decayed and instead interact with the next pressure waves being generated. Lower frequencies limit droplet ejection rate, and can also inhibit

droplet formation if the frequency is so low that a proper acoustic state within the nozzle is not established. The rate of wave decay is strongly dependant on ink composition. In particular, increased viscosity results in shorter decay times due to damping effects.

Lastly, the length of the fluid cavity can influence the droplet formation process. This length has an impact on four important parameters, some already highlighted. These include optimum pulse width, period of meniscus oscillation, period of low frequency resonant and anti-resonant synchronous operation [65].

2.2 Fluid Rheology

Drop-on-demand printing is a very precise and finely tuned physical process which is heavily dependent on the properties of the fluid to be dispensed. Rheological properties dramatically affect the ability to generate droplets; indeed, if fluid parameters do not fall within a well-defined range, droplet generation is impossible. However, it is of importance to keep in mind that the droplet generation process is not yet completely understood and remains a heavy area of research. Furthermore, the vast majority of studies conducted so far have been done using Newtonian fluids; the dispensing of non-Newtonian fluid such as particle suspensions and polymers is a relatively new development. With that in mind, the fluidic physical properties which are known to affect fluid flow and droplet generation will be discussed here. The key bulk fluid parameters important for inkjet dispensing include viscosity and surface tension. Boiling point of solvents can also be important due to effects of precipitation at the nozzle orifice [67]. Boiling point, however, was not characterized in this work.

2.2.1 Viscosity

The viscosity of a solution is its resistance to deformation. Shear stress between different flow layers traveling at different velocities leads to resistance to applied force. Solution viscosity has major implications for inkjet printing. The rate at which the acoustic waves generated by piezoelectric actuation attenuate is directly proportional to viscosity [68], and can be described as

$$\propto = \frac{2\eta\omega^2}{3\rho_f c^3}, \qquad \textbf{2.1}$$

where $\propto$ attenuation, η is dynamic viscosity, ω is the sound frequency, ρ_f is the fluid density, and ψ is the speed of sound. When using a unipolar pulse, droplet ejection depends on the transfer of sufficient kinetic energy to the fluid air interface in order to overcome surface tension; enhanced rates of wave results in less energy being transferred. As compensation, higher driving voltages are required to generate sufficient energy and eject solutions of increasing viscosity. We utilized MicroFab nozzles in this work, which are capable of ejecting solutions with a maximum viscosity of 20 mPas, which is dictated by the voltages the nozzle can withstand as well as its internal geometry. Viscosity itself does not affect the speed of the wave; however, density does. The speed of sound within a fluid is given by the following relation,

$$c = \sqrt{\frac{P}{\rho_f}}, \qquad \textbf{2.2}$$

where c is the speed of sound, P is the bulk modulus, and ρ_f is fluid density.

It should also be noted that the presence of particles in solution (such as was the case in this work) may also affect solution viscosity by the following relationship,

$$\eta = \eta_o(1 + A\Phi), \quad \textbf{2.3}$$

where η is the viscosity of the suspension, η_o is the viscosity of the carrier fluid, Φ is the volume fraction of the particles, and A is a physical constant which is related to the shape of the particles [69].

2.2.2 Surface Tension

The orifice of the nozzle lies at the fluid and air interface [63]. The surface tension that is present at this interface is what dictates the amount of wave energy required for droplet ejection. Surface tensions of inkjet inks are finely tuned. The amount of kinetic energy transferred by the pressure wave must be greater than the surface energy required to form a drop. Care must be taken to ensure surface tension is not so high that it impedes droplet formation. The theoretical minimum droplet velocity needed for drop ejection can be derived from this surface tension as follows,

$$v_{min} = (\frac{4\gamma}{\rho_f d_n})^{1/2} \quad \textbf{2.4}$$

where d_n is the nozzle diameter, ρ_f is the fluid density, and γ is the surface tension. For a nozzle diameter of approximately 100 μm, the minimum velocity is on the order of several meters per second [66, 70].

Lastly, fluid properties also influence how a droplet impacts a substrate, as well as how the fluid spreads once impact has been made. Furthermore, these properties will also govern the evaporation behaviour and the manner in which the solute is deposited on the substrate. This ultimately affects the features of the resulting pattern. These behaviours are complex and will not be detailed here, as this work did not explore these particular

phenomena. The reader is referred to several papers outlining the process and its impact for experimental fluids [61, 71].

2.3 Cell Suspension Rheology and Influencing Phenomena

Inkjet systems have traditionally been used with homogeneous, well dispersed fluids. Effective inkjet performance hinges on consistent rheological behaviour throughout the duration of operation. This work focused on the delivery of experimental cell based suspensions using a piezoelectric system. Ideally, particles within experimental fluids should be small and well dispersed [72]. However, the cells present in these suspensions are of a size sufficient enough that they undergo the influence of various physical forces and phenomena while in an inkjet setting. These include, but are not limited to, gravitational, lift and buoyant forces, as well as inertial influences. Adding to the complexity are the intrinsic properties of the cells themselves; they are prone to aggregation. The presence of protein molecules, such as cadherin and integrin, on the surface of cells causes them to interact with one another [73, 74] and form multicellular clusters in suspension. Ultimately, the combination of these influences results in a dynamic remodelling of cell suspensions over time, which has profound negative consequences on inkjet performance. We herein provide a theoretical background detailing these influences.

2.3.1 Gravitational Force

Particles within a suspension will be subject to gravitational influences. These particles will experience gravitational force (weight) in the direction of gravitational acceleration. The gravitational force can be defined as,

$$F_g = mg, \tag{2.5}$$

where F_g is the magnitude of the gravitational force, m is the mass of the object, and g is gravitational acceleration. This can be further redefined in terms of the particle density (ρ_p) and volume (V) of the object as

$$F_g = \rho_p V g. \tag{2.6}$$

2.3.2 Buoyancy

Any particle completely submerged in a fluid will experience a force of buoyancy. Buoyancy is defined as the upward force exerted by a fluid on an object which opposes the weight of the object. Any object submerged in a fluid displaces a volume of fluid equal to the volume of the object. The weight of the displaced fluid can then be calculated, by knowing the density of the fluid as well as the volume displaced. The buoyancy force can then be defined as

$$F_b = \rho_f V g, \tag{2.7}$$

where ρ_f is the density of the fluid, V is the volume displaced, and g is gravitational acceleration. By combining the equations for gravitational and buoyant forces, we arrive at the following relationship which defines the effective gravitational force as

$$F_{net} = (\rho_p - \rho_f) V g, \tag{2.8}$$

where F_{net} is the effective gravitational force, ρ_p is the particle density, ρ_f is the fluid density, V is the volume, and g is gravitational acceleration.

Particles undergoing sedimentation in a fluid also experience an equl drag force acting in the opposite direction of relative motion, defined generally by Stokes' Law as

$$F_D = 6\pi\mu R v_{sed}, \quad \textbf{2.9}$$

where F_D is the frictional force acting between the fluid and particle, μ is the dynamic viscosity (Ns/m^2), R is the radius of the spherical object (m), and v_{sed} is the particle's settling velocity (m/s). By equating the effective gravitational force and the drag force, the settling velocity of particles in fluid can be derived as the following relationship,

$$v_{sed} = \frac{(\rho_p - \rho_f) g {D_p}^2}{18\mu}, \quad \textbf{2.10}$$

where v_{sed} is the sedimentation velocity, g is the gravitational acceleration, D_p is the particle diameter, ρ_p and ρ_f are the particle and fluid densities respectively, and μ is the fluid viscosity. This relationship is used later on for theoretical analysis.

2.3.3 Lift Force

A particle moving within a flow will experience a lift force in direct proportion to its relative velocity compared to the velocity of the fluid. The flow will exert a force on the projected area of the particle; the component of this force perpendicular to the flow direction is termed lift. This lift force will also depend heavily on the density of the fluid as well as the projected area as follows,

$$F_L = \frac{1}{2} C_L \rho_f {v_p}^2 A, \quad \textbf{2.11}$$

where C_L is the lift coefficient, ρ_f is the density of the fluid, v_p is the velocity of the particle, and A is the projected area. If the forces are great enough that differences exist between particle and fluid velocity, an opposing drag force will also be created, defined as

$$F_D = \frac{1}{2} C_D \rho {v_p}^2 A, \quad \textbf{2.12}$$

where C_D is the drag coefficient. Lift forces and opposing drag forces can provide a means to account for observed particle trajectories in fluidic pathways.

2.3.4 Inertia

Inertia is defined as follows,

$$F_p = ma, \quad \textbf{2.13}$$

where F_p is the net force imposed on the particle, m is the mass of the particle, and a is the acceleration of the particle. This net force can be expressed as a sum of the previously defined forces as

$$\overrightarrow{F_p} = \overrightarrow{F_g} + \overrightarrow{F_b} + \overrightarrow{F_L} + \overrightarrow{F_D}, \quad \textbf{2.14}$$

where $\overrightarrow{F_g}$ is the gravitational force, $\overrightarrow{F_b}$ is the buoyant force, $\overrightarrow{F_L}$ is the lift force and $\overrightarrow{F_D}$ is the drag force. By accounting for all of these influences on a particle we can begin to see how particles found in different locations within systems such as a piezoelectric inkjet printer may follow different flow trajectories. The magnitude of local forces will dictate the behaviour of particles in that region.

The magnitude of these forces is also dependent on the diameter of individual particles. Complicating this behaviour is the fact that the particles we worked with, cells, interact with one another. Issues associated with this fact are discussed below.

2.3.5 Biological Factors

In this work, MCF-7 breast cancer cells were used for all experiments. MCF-7 cells express high levels of cadherin proteins on their surface, which are responsible for cell to cell attachment [75, 76]. Close proximity of cells may result in high levels of interaction compared to inert particles where no interaction other than elastic collision is expected. Cancer cells are also deformable, which impacts how these experience forces within a fluid stream. In particular, deformable objects experience additional lift force proportional to the extent of their deformability. Inertial microfluidic techniques have been successful at classifying cells by their lateral migration within microfluidic channels, based on this additional force [77].

Furthermore, the interaction of cells will lead to the formation of multicellular clusters of various sizes, altering size distribution. This distribution of particle size is known to be important for micro channel cluster formations [78]. Multicellular clusters of varied sizes would experience varied magnitudes of the previously described forces when compared to a single cell. For example, drag force is directly related to particle radius, and sedimentation rate is directly related to particle diameter. As a result, a cell suspension will display a variety of particle behaviours based on size, and these behaviours will change over time as aggregates continuously form. Aggregates were apparent during this work; an example of a large aggregate within the nozzle is shown in Figure 2.4.

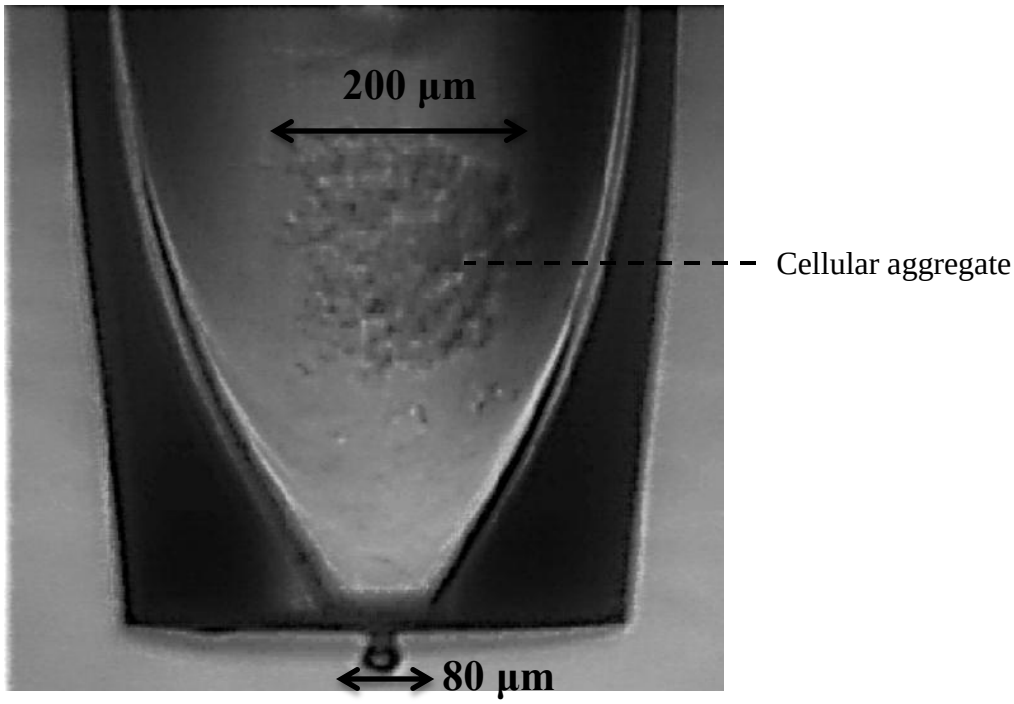

Figure 2.4. Photograph of a large cellular aggregate (200 µm) present in the inkjet nozzle. Although exact number of cells cannot be determined from this photo, this cluster appears to be composed of several hundred to several thousand cells.

2.4 Relevant Phenomena within an Inkjet Nozzle

The combination of physical and biological parameters within fluid flow raises areas of key concern. Different points within the inkjet system impart varying magnitudes of forces of interest on particles within the flow. Particle trajectories resulting from these net forces can lead to undesirable effects such as deposition, cluster formation, and disturbance of the overall dispersion. Particular situations are discussed here.

2.4.1 Inertial Impaction – Particle Deposition and Cluster Formation

An inkjet system consists of many points where the fluid flow direction is quickly re-oriented. Examples where such behaviour occurs includes changes in tubing direction as well

as the rapid convergence of walls within the nozzle. If the change in the direction and magnitude of the fluid flow is large enough, the net force imposed on the particle may cause it to deviate from established fluidic streamlines. If near a channel wall or junction, the particle may collide with the nearby structure and deposit. This phenomenon is known as inertial impaction [79]. The deposition of an initial particle will serve as a seed event for further buildup. These buildups become quite problematic in fluidic systems; the flow of fluid can be re-oriented and further buildup can eventually cause full blockage of channels [80]. A depiction of how a particle may impact with walls is shown in Figure 2.5.

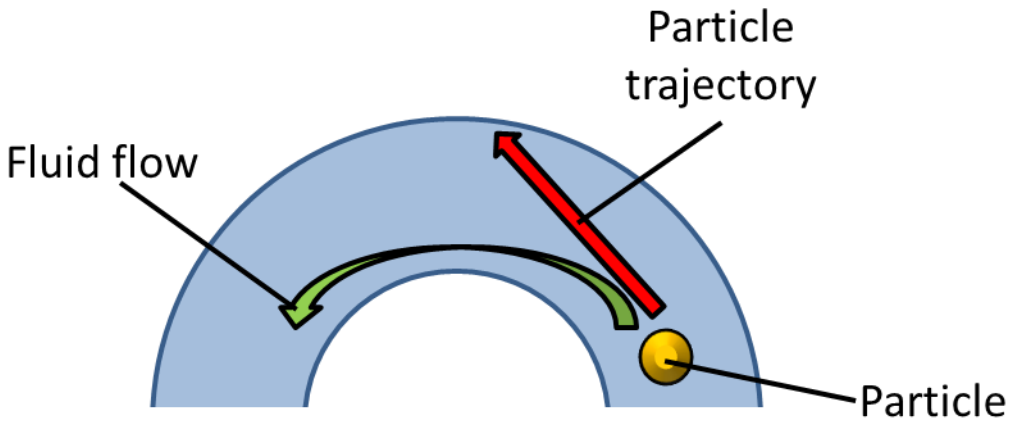

Figure 2.5. Inertial forces experienced by a particle as it travels through a channel rapidly changing direction may cause the particles to deviate from fluid streamlines. The green arrow represents the path of the fluid, whereas the red line represents the path of the particle. Collision with the wall may cause particle deposition and formation of larger cellular clusters that may impede inkjet performance.

2.4.2 Region near the Orifice

Another crucial area where such impaction and buildup may occur is within the nozzle near the orifice. Based on Figure 2.6, the internal geometry of the nozzle quickly

converges from the capillary diameter of 350 μm to the orifice diameter of 80 μm. This convergence occurs over a distance of 300 μm. In addition to potential particle impaction due to inertial consequences, the orifice is also the region of largest shear within inkjet systems. This results in large shear induced lift forces present at this point, which may also contribute to the deposition of cells along channel walls. Furthermore, cells themselves are of diameter 10 to 20 μm, which is relatively large compared to the orifice diameter. Clogging formation in three-dimensional suspension flows through sudden contractions has been hypothesized to depend on this ratio of particle diameter to channel diameter [78]. Lastly, the symmetrical geometry of nozzle convergence may pose a problem at this magnitude of particle to channel diameter ratio. Channel symmetry has been observed to be a factor in blockage; particles converge in a symmetrical manner from multiple sides of the channel, impact each other, and then subsequently deposit and cause blockage of the channel junction. Asymmetrical channel design has been shown to reduce this phenomenon [81]. Lastly, sedimentation of particles when the nozzle is not operating may cause these particles to deposit. Deposition of particles through these various means near the nozzle orifice poses the potential to negatively impact the drop formation process, causing changes in drop directionality, and may halt the entire process itself through blockage.

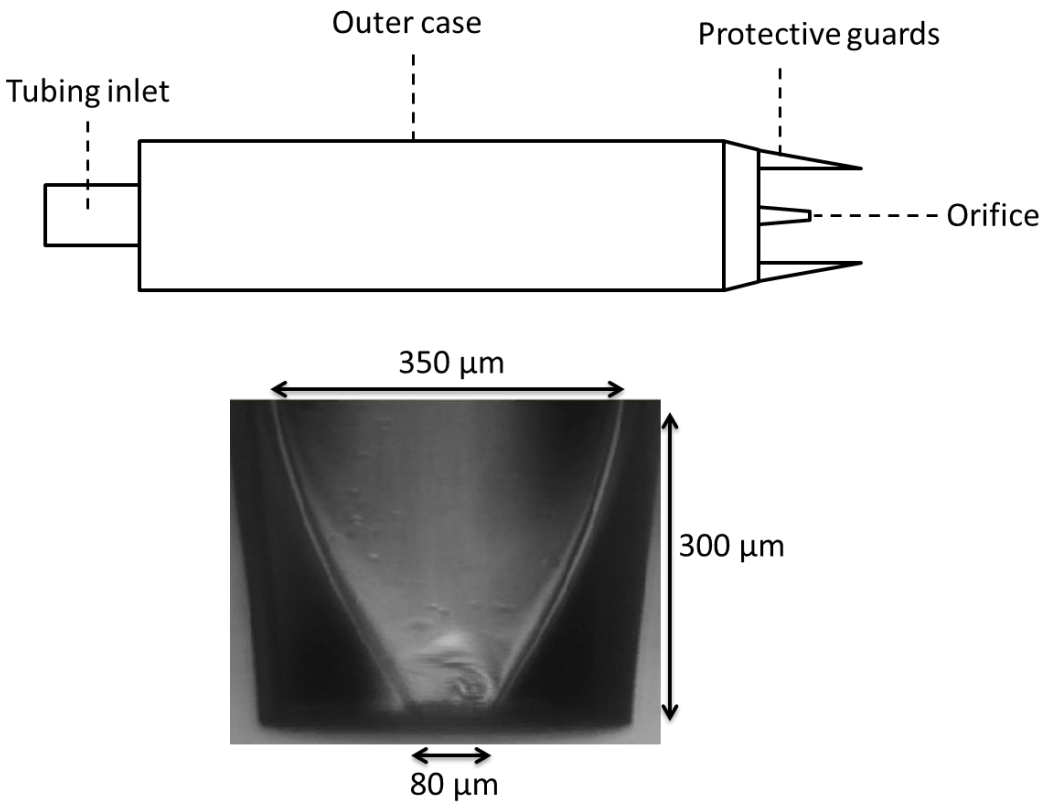

Figure 2.6. A schematic of the MicroFab inkjet nozzle, as well as a camera image of the nozzle tip displaying dimensions near the orifice. The nozzle used in this study had an orifice of 80 µm diameter.

2.4.3 Sedimentation

Gravitational force is present at all points in an inkjet system. In addition to the nozzle, gravitational influence is present on particles moving through fluidic pathways, as depicted in Figure 2.7. Sedimentation of particles due to gravitational influence may result in non-uniform concentrations of particles throughout the entirety of the fluid volume.

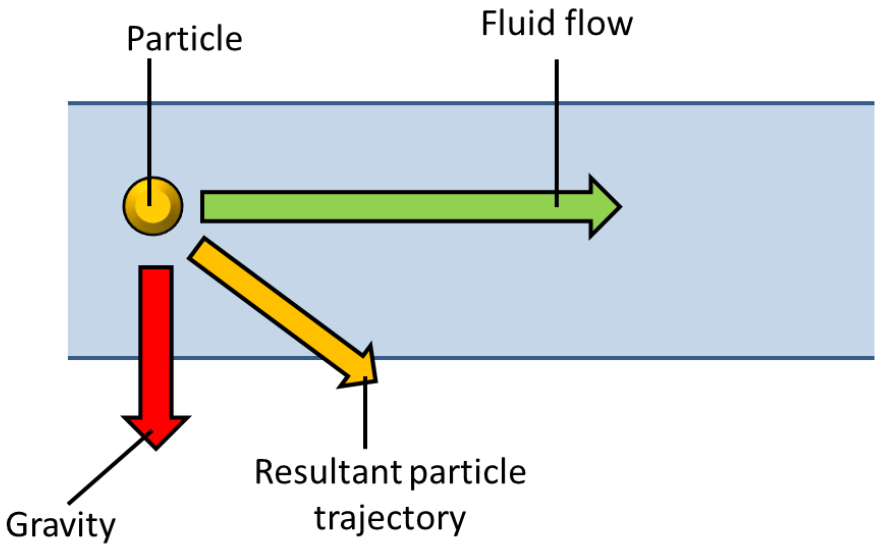

Figure 2.7. The influence of gravity on a particle traveling through a channel. Gravity (red) will pull the particle away from the streamline (green). The orange arrow depicts the resultant path. This influence will differ based on the directions of the channel / streamline relative to the direction of gravity. Such influences can lead to deposition and formation of cellular clusters.

Of much greater concern, however, is the situation that is found within the fluid reservoir. The influence of fluid flow into the tubing is localized to its immediate vicinity. Cells that do not fall into this immediate vicinity will sediment out of the tubing's range and fail to enter the fluid flow being transported to the nozzle. Over time this leads to particles not being delivered to the nozzle for dispensing. This situation is shown is Figure 2.8.

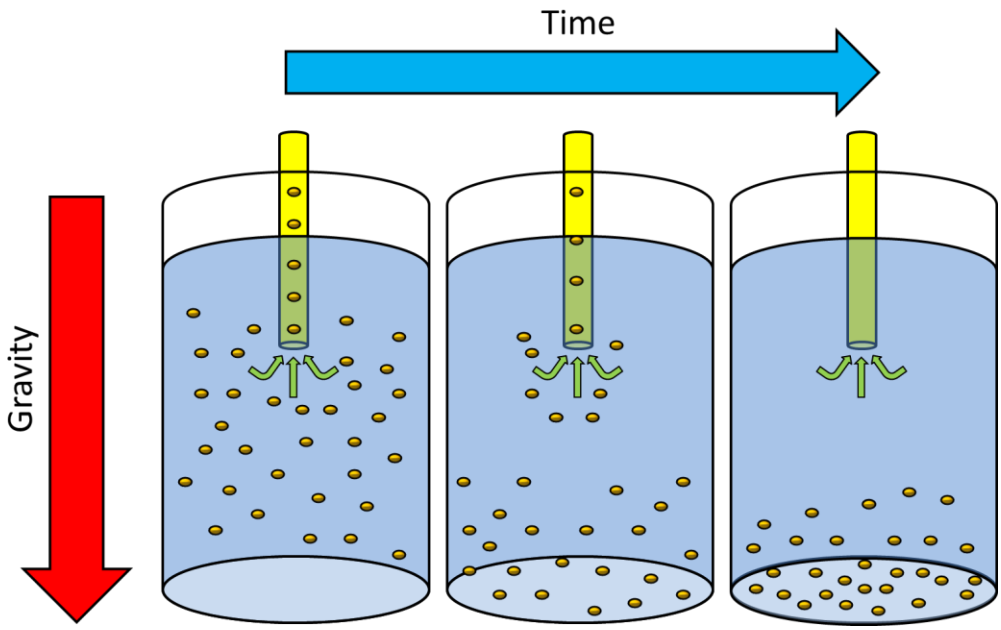

Figure 2.8. Sedimentation of cells within the fluid reservoir. Cells in the immediate vicinity of the tube intake can be drawn into the tubing which supplies the nozzle. Over time, this sedimentation in the reservoir will lead to a build-up of cells near the bottom of the reservoir, with a negligible amount of cells being drawn into the tubing for dispensing.

This segregation of particle concentration poses fundamental challenges for the inkjet dispensing process. If a constant amount of particles are not being dispensed as operation continues, any advantages associated with small volumes are lost. Indeed, appropriate techniques to maintain appropriate particle (cell) dispersion are required for such applications. Methods such as intra-reservoir stirring have failed to address this issue, suggesting that appropriate means of controlling dispersion and preventing particle deposition are needed throughout the entirety of the system [82]. In this thesis, we have proposed a rheological means of addressing this problem, which is discussed in Chapter 3. We propose the hypothesis that mitigation of cellular sedimentation within the fluid will result in a more accurate and reliable inkjet cell dispensing process.

Chapter 3: Cell Suspension Formulation

Ink formulation is a critical aspect of inkjet dispensing technologies [83]. Fluid parameters must be in a narrow range compatible with inkjet technology. In particular, surface tension must be low enough to enable droplet formation, and viscosity must not exceed a threshold limit. Traditional inks display such values, for example, the original inks used for Epson printers exhibited viscosities of 2 – 6 mPa•s and surface tensions of 30 – 34 dyn / cm^2 [84]. Experimental fluids may not be as ideal, and modification may be required. However, these materials pose additional challenges such as undesired chemical reactions. For example, although the additives used in conventional inks can accomplish the fine tuning of viscosity and surface tension, these additives cannot be utilized with experimental materials such as polymers because they will affect the polymer performance [66].

In the case of cellular suspensions, several issues are raised. One must find a way to mitigate cellular aggregation, sedimentation, and deposition in order to improve inkjet performance. However, any additives should not increase the suspension viscosity above the printable range (20 mPa•s for the MicroFab nozzles used in this study). Also, cellular viability must not be sacrificed in order to achieve these goals. All applications of this technology are dependent on the fact that cells are capable of further growth and division after dispensing, and are capable of being processed using downstream assay technologies. This chapter details requirements that must be considered to ensure cellular viability and improved inkjet performance. Potential additive agents to accomplish these goals are discussed, as are concerns associated with these additives. Lastly, a basic theoretical model is presented and used to establish appropriate experimental conditions.

3.1 Cellular Requirements

Cell culture media exists to enable the maintenance and growth of cells. Media formulations will vary with cell type, which often take form in differences in pH, glucose concentration, growth factors, salts, and other nutrients. Growth factors are derived from animal blood, such as fetal bovine serum (FBS). Overall, cell culture formulations remain quantitatively ill-defined [85], which may be problematic for technological applications such as inkjet printing. However, cells require such media formulations in order to remain viable and intact for further downstream assays. In order to ensure cell viability throughout the entirety of the printing process, all suspensions in this work were created using a base of standard cell culture media (Dulbecco's Modified Eagle Medium, Invitrogen), which has a viscosity of approximately 4 mPa•s, as found in this work.

Another parameter of importance is that the cells used in this study, MCF-7 breast cancer cells are an adherent cell type. Adherent cells are those which require attachment (usually to a surface) for survival. Attachment to a surface is usually needed before other assays can be carried out. Such a surface can either be tissue culture plastic, or a micro carrier in the case of bioreactors. Additionally, MCF-7 cells can grow as spheroids through attachment to other cells or to basement membranes such as particular protein structures [86]. Attachment to surface can only be accomplished if cells sediment to the bottom of the specified chamber and come into contact with the flat surface. However, in a dispensing system, sedimentation within the fluid results in inadequate particle dispersion. Therefore, in order to accomplish reliable printing, one must mitigate the sedimentation of cells whilst they are within the inkjet system, but allow for their attachment once dispensed. Attachment can be accomplished, for example, by dispensing cells into a chamber pre-filled with fluid which

effectively dilutes the concentration of anti-sedimentation (high density) compounds. Cells must also remain viable for as long as they remain within the system. Furthermore, any additions that reduce aggregation tendencies need to be assessed for their impact on biological function.

3.2 Reduction of Sedimentation through Ficoll-PM400

Reducing or eliminating particle sedimentation within fluids can be accomplished by raising solution density to the point where the particles are neutrally buoyant in the fluid. In that regard, additives that increase solution density, preserve cellular function, and stay within the viscosity threshold of piezoelectric inkjet printers would be ideal.

Density based cell separation is a widely used technique with an established history [87]. Briefly, linear or discontinuous gradients of polymer solutions are created and loaded into centrifugation tubes. Cells isolated from various tissues are then placed within these tubes. Centrifugation of these tubes results in cells migrating to where the gradient density matches their own. In this manner, cells of different densities can be separated layer by layer.

One of the commonly used compounds for cell separation is known as Ficoll. Ficoll is a highly branched, high molecular weight sucrose co-polymer that is formed by the polymerization between sucrose polysaccharide and the organochlorine epoxide Epichlorohydrin. Ficoll molecule radii range from 4 to 7 nm. The high degree of molecular branching, as well as the large hydroxyl group content, ensures good solubility in aqueous media. Additionally, Ficoll does not contain any ionized groups ensuring that no reactions will occur with salts or biological compounds. Lastly, the intrinsic osmolality of Ficoll is low when compared to sucrose at equivalent concentrations; this results in preservation of the

physiological and morphological integrity of cells. In addition to its use in density gradients, Ficoll is used for a variety of biological applications including organ preservation, molecular stabilization, and surgical procedures [88]. It should be noted that this work utilized the Ficoll PM400 derivative for all experiments, which is depicted in Figure 3.1.

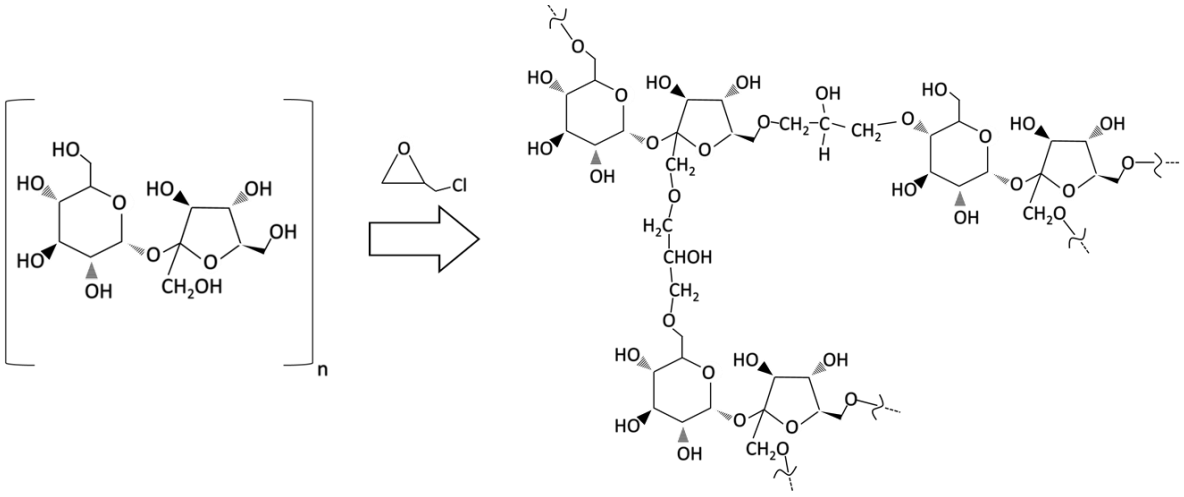

Figure 3.1. The chemical structure of the Ficoll co-polymer. Sucrose can be cross linked to create Ficoll co-polymer in the presence of epichlorohydrin. Ficoll is highly branched and chains can extend from a number of points as indicated by dashed lines; the right hand side of this reaction displays only a portion of the total structure. The number of side chains and degree of polymerization can be varied to create polymers of different molecular weight. In this study, we utilized the higher molecular weight derivative (Ficoll-PM400).

An interesting property of Ficoll polymer is its low intrinsic viscosity. Similar compounds used in gradient separations, such as dextran, display much higher viscosity values at similar concentrations. This proves to be highly useful for our application of piezoelectric inkjet printing. The use of Ficoll as an additive to cell suspensions provides the opportunity to increase suspension density to the point of neutral buoyancy while keeping

viscosity low enough that it does not exceed the inkjet threshold. Densities and viscosities as a function of Ficoll concentration are shown in Figures 3.2 and 3.3.

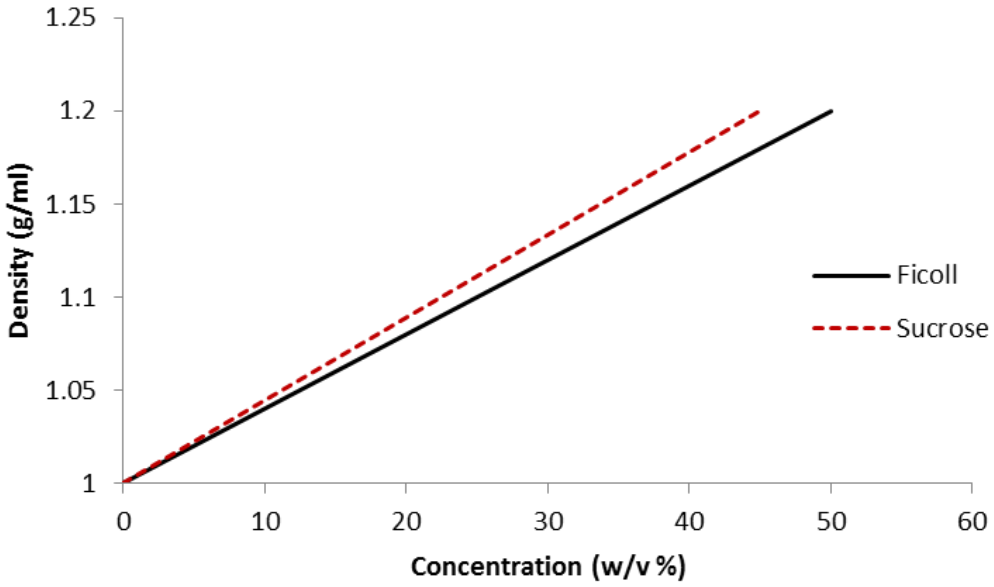

Figure 3.2. Densities of Ficoll PM400 and sucrose solutions as a function of concentration. The two compounds display similar density values, however, Ficoll's intrinsic osmolality is much lower. This makes it suitable for cell culture applications. Adapted from [88].

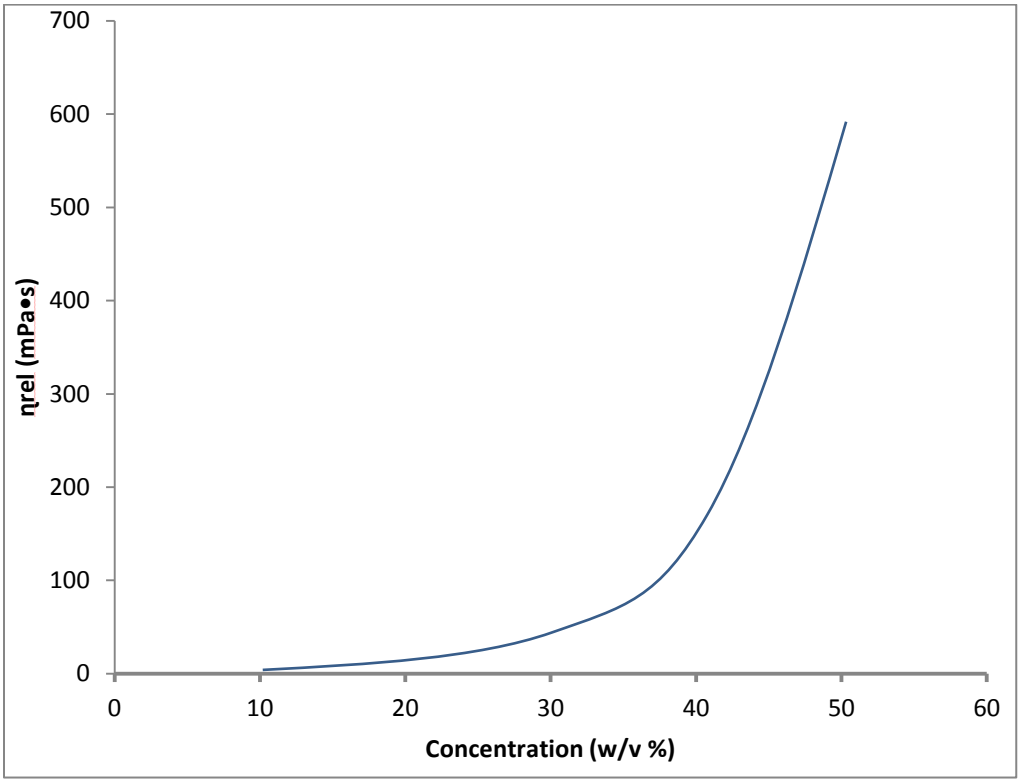

Figure 3.3. Relative viscosity of Ficoll PM400 solutions at different concentrations. Hypothetically, concentrations of 20% should be attainable without exceeding the inkjet threshold of 20 mPa•s. Relative viscosity refers to the ratio of the viscosity of the solution to the viscosity of the solvent used. Adapted from [88].

3.3 Pluronic-F127 for Surface Tension Reduction

Surface tension opposes droplet formation. In order for a droplet to be ejected from the orifice of the nozzle, the generated pressure wave must transfer a larger amount kinetic energy outwards than the surface energy needed to form a drop. For solutions that require larger amounts of energy for drop formation, kinetic energy may be increased by increasing the amount of voltage applied. Additionally, one may also reduce the surface energy that is present at the meniscus by decreasing surface tension. As the addition of Ficoll to solution

increases viscosity in addition to density, such surface tension modification proves to be a useful tool.

Pluronic-F127 is a non-ionic, surfactant tri-block co-polymer that is used to facilitate solubilization of various materials into physiological media [89]. It accomplishes this through reduction of surface tension. We have incorporated Pluronic-F127 into cellular suspensions in order to aid droplet generation at the orifice. Although this compound is capable of disrupting cellular membranes, the low concentration of 0.05% used in our experiments is non-toxic to cells [90].

3.4 Theoretical Model of Sedimentation

In order to aid our experimental design, a simple theoretical model of cellular sedimentation was generated. The model was used to decide which Ficoll concentrations would result in neutral buoyancy. Also, these theoretical results served as a benchmark to which we could compare our experimental observations.

Sedimentation velocity depends on a number of variables, including fluid density, particle density, effective particle diameter, and viscosity. Fluid density and viscosity values will increase as Ficoll concentration is increased. Particle density refers to the density of a cell. The direct mass measurement of cells is a very recent technological advance [91], however, MCF-7 density has been determined by other means. Griwatz and colleagues used Nycoprep density gradient centrifugation and radioactive [3H] thymidine-labelling, and determined MCF-7 cell density to be 1.068 g/mL[92]. Such techniques have been known to give slightly varying results [93]; however, the numbers serve as a good benchmark.

Effective particle diameter is also of key concern. Aggregation of cells will lead to particles of larger diameter (e.g. a cluster of two cells has a larger effective particle diameter than a single cell), which will result in an increased sedimentation velocity. In an experimental setting, the range of sedimentation velocities will vary due to such aggregation. Therefore, averaged measurements will display a result which is representative of these combined velocities at any given point in time.

For our model, we generated curves predicting the sedimentation velocities of cells as a function of increasing Ficoll concentration. Curves were generated based on equation 2.10. Curves representing the sedimentation of a single cell with diameter D_p, a particle with diameter $\sqrt[3]{2}D_p$ (this cluster has 2 times the volume of a single cell) and a particle with diameter $2D_p$ (this particle has 8 times the volume of a single cell and represents a cluster of cells) are displayed. The curves are detailed in Figure 3.4.

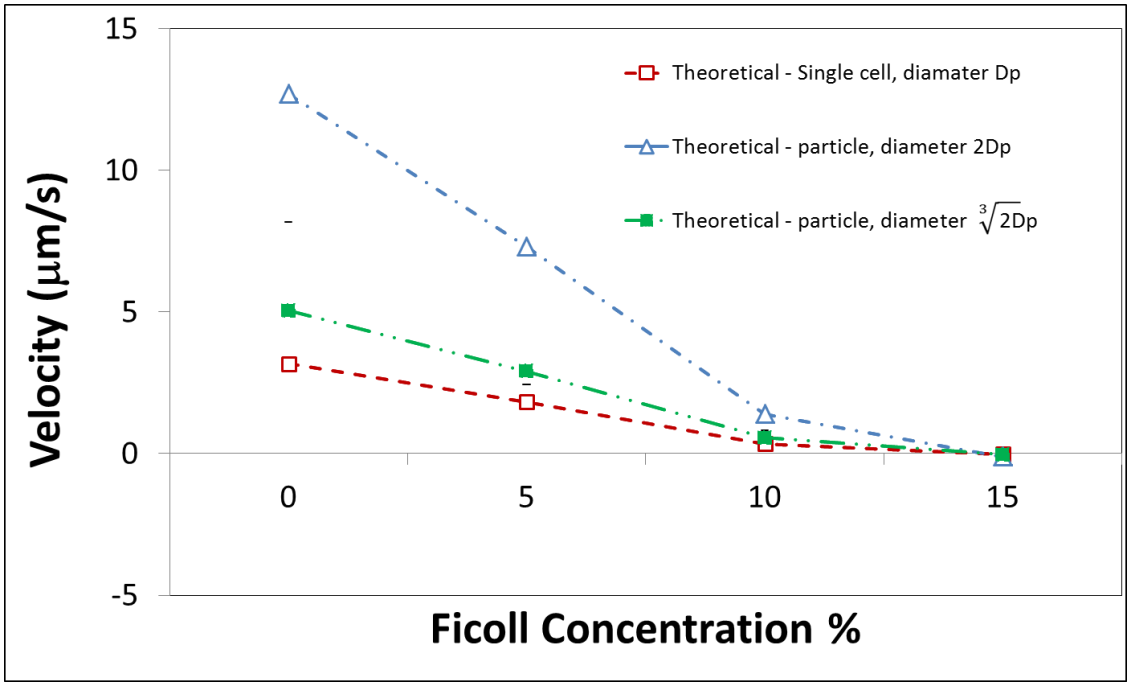

Figure 3.4. Theoretical curves for the sedimentation velocity of single cells with diameter $\boldsymbol{D_p}$, a particle which has twice the volume of a single cell (diameter $\sqrt[3]{\boldsymbol{2}}\boldsymbol{D_p}$), and a particle with diameter $\boldsymbol{2D_p}$ (this particle has 8 times the volume of a single cell). These curves were generated based on the settling velocity equation (equation 2.10) derived from Stokes' Law as well as the estimated concentrations of Ficoll to be used.

Chapter 4: Experimental Results and Discussion

This chapter focuses on the experimental results of our attempt to characterize and correct issues associated with improving the reliability of cellular inkjet printing. Ficoll-PM400 was used to create neutrally buoyant cell suspensions. To ensure cellular compatibility, cell viability was first characterized after extended periods of suspension. Viscosities of Ficoll-PM400 based suspensions were measured to ensure that inkjet printing was a feasible means of dispensing. Sedimentation velocities of cells within suspension were characterized using digital video microscopy. Reliability of the inkjet system was assessed using time-lapse dispensing and CyQuant assays.

It should be noted that most of the Figures that follow can be found in reference [94].

4.1 Cellular Viability

MCF-7 breast cancer cells, the cells which were used for all experiments in this thesis, are an adherent cell type. They require attachment to a surface in order to grow and divide. We attempted to improve inkjet performance by making cell suspensions neutrally buoyant during the printing process. Although concerns about cell attachment post printing can be addressed by dispensing into a reservoir already filled with liquid (which effectively dilutes Ficoll concentration and allows for cells to sediment), we had to confirm that suspension for the duration of printing did not affect cellular viability. We accomplished this analysis through suspension for a specified period of time, followed by dilution and plating of the cells. Cells were assessed for viability 48 hours after this step using an MTT (3-(4, 5-Dimethylthiazol-2-yl)-2, 5-diphenyltetrazolium bromide) colorimetric assay. MTT is a

yellow tetrazole, which is reduced to purple formazan in living cells. The reduction is accomplished by dehydrogenases and reducing agents present in the cell, as depicted in Figure 4.1. The MTT formazan product is thought to correlate directly with the number of living cells [95].

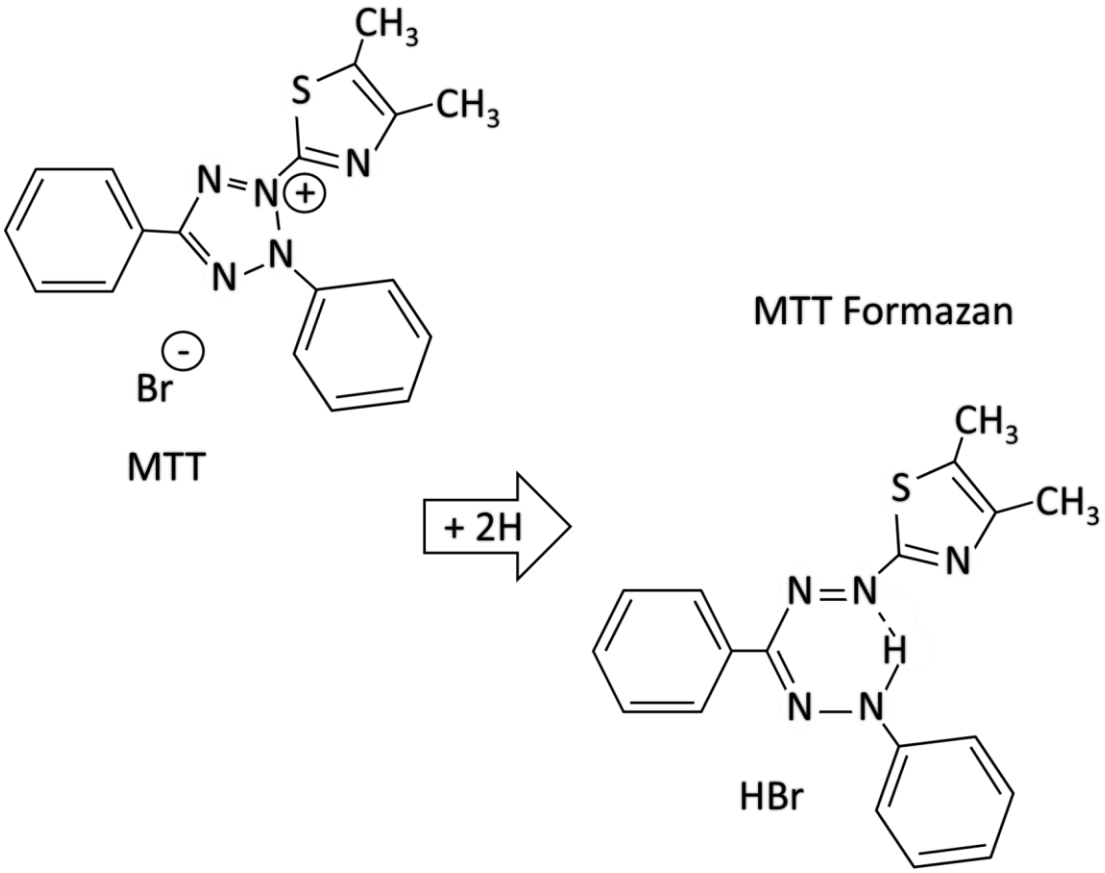

Figure 4.1. The reduction of MTT to MTT Formazan.

4.1.1 Experimental Details

MCF-7 cells were propagated in DMEM media supplemented with 10% FBS as previously outlined. Cells were washed with PBS and detached through the use of trypsin. Cell counts were assessed through trypan blue dye staining and the use of a haemocytometer. Cells were diluted to a concentration of 500,000 per mL using both standard DMEM media

(with 10% FBS) as well as the desired amount of Ficoll-PM400 (in DMEM media) stock solution. Suspensions at this cell concentration were made with Ficoll concentrations of 0%, 2.5%, 5%, 10%, 15% and 20%. These suspensions were left to rest for 1hour at room temperature in an attempt to simulate a suspension that would be found in a printing reservoir. Our rationale for assessing viability in this manner rather than direct assessment after printing was so that we could decouple the effects of printing from those of suspension. A one hour period was deemed long enough to demonstrate proof of concept. Longer wait periods may be of interest for future work. After the wait period was completed 10,000 cells (20 μL) of each suspension were pipetted into wells of a 96 well plate and diluted with 200 μL of DMEM media to allow cellular sedimentation and attachment. Each suspension was assessed in triplicate (at minimum). Cells were then incubated at 37^0C, 5% CO_2 for 24 hours, at which point all media was replaced with fresh media in order to eliminate all traces of Ficoll polymer. The cells were incubated again for 24 hours at which point 100 μL of MTT reagent was added to each well. Also, MTT reagent was added to wells lacking cells in order to serve as a control. Cells were incubated in the presence of MTT reagent for 3 hours, in order to allow ample time for digestion. Upon completion, all reagents are removed from the wells, leaving only the stained cells. DMSO (dimethyl sulfoxide) is an organosulfur compound that is used to solubilize the cells; 100 μL was added to each well and solutions were shaken gently for 5 minutes. Absorbance spectroscopy measurements were then taken using a Biomek DTX 880 multimode detector (Beckman Coulter). An absorbance wavelength of 595 nm was used for measurements. All measurements were normalized to the 0% control suspension for a relative comparison in an attempt to determine whether Ficoll polymer had an effect on viability.

4.1.2 Results

Previous work by several groups has demonstrated the feasibility of using inkjet systems to deliver cell suspensions. Furthermore, cells have been shown to survive the process [38, 40, 46]. Work from our group has already shown the retention of cellular viability using our current piezoelectric inkjet system [90]. Briefly, HepG2 hepatocytes were both pipetted and printed into wells containing gelled collagen, and viability was assessed over the course of 7 days using Calcein-AM / EthD-1 stains. It was found that printed cells maintained similar viability to the pipetted cells over 4 days, although viability of printed samples was less after 7 days. Regardless, this study demonstrated that dispensing using our piezoelectric inkjet system does not decrease cell viability over the first 4 days of culture when compared to manually pipetted cells. Figure 4.2 showing that residence times up to one hour in a neutrally buoyant, Ficoll based culture media solution have no adverse effects on MCF-7 cell viability.

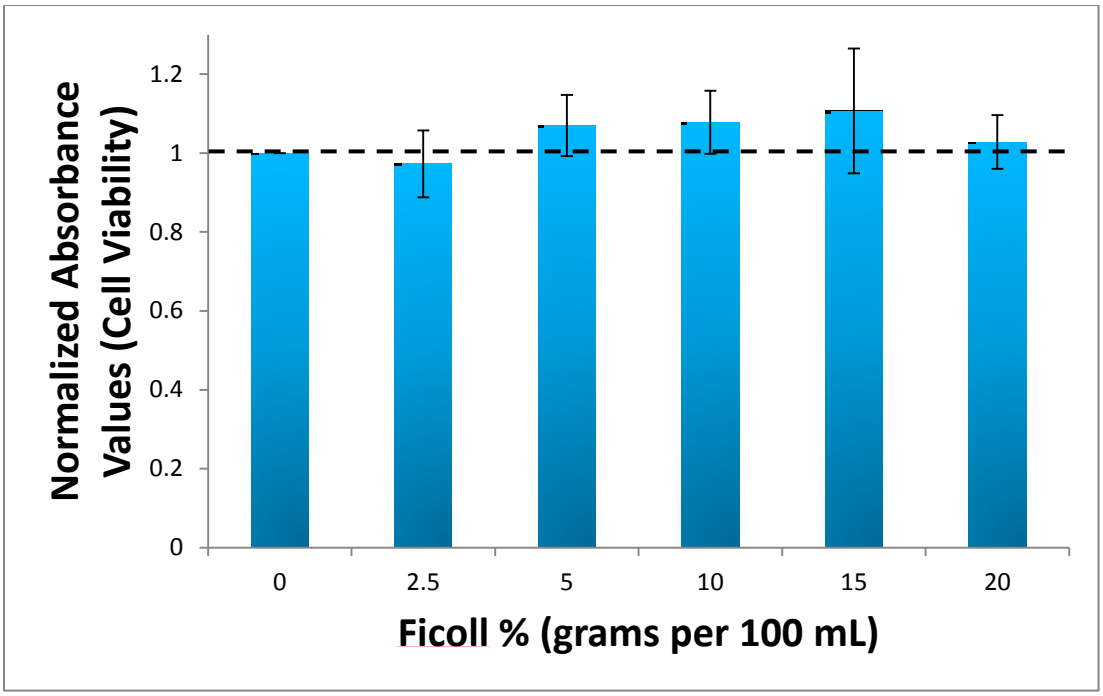

Figure 4.2. Cellular viability after 1 hour of incubation in Ficoll based suspensions. A cell concentration of 500,000 / mL was used for all experiments. Absorbance measurements were accomplished using a MTT assay. All values are normalized to the 0% solution. The dashed line represents the normalized value of 1. All values fall within the range of error.

The dashed line in Figure 4.2 represents the normalized control value. This reference sample consisted of an initial seeding of 10,000 cells which had not been suspended. The normalized absorbance values for Ficoll concentrations of 2.5%, 5%, 10%, 15% and 20% (w/v) were 0.97, 1.06, 1.08, 1.11 and 1.02, respectively. These results demonstrate that neutrally buoyant cell suspensions can be utilized for printing applications without effect on cellular viability.

Cellular viability is a key concern when using dispensing systems. Cells are subjected to potentially harmful phenomena within these systems, which has led many to question whether inkjet dispensing of cells will ever be a promising approach for cell patterning. High

shear stresses found at the nozzle tip, the generation of heat in thermal systems [96], the pressure wave experienced by the cells, and the impact experienced by cells once a droplet makes contact with a surface [97] have all been implicated as concerns for cellular viability. Some of these processes have been examined, for example, shear stresses up to 500 kPa generated at the orifice by increasing pressure have been found to be a larger concern for cell viability than the size of the orifice [98]. Heat generation has actually been exploited to open up cellular pores and transfect the cells with DNA reagents during the printing process [40]. Exposure to the air environment has been addressed by printing into "bio-paper"; gel environments such as collagen [99]. It should be noted that even with these innovations, cell viability will differ for different cell types. As such, comprehensive analysis of each type will be needed in order to determine optimal printing conditions. Nonetheless, the ability of these cells to withstand these conditions provides a promising outlook for utilization of this technology.

4.2 Viscosity Characterization

Viscosity arises from resistance to deformation by shear stress. The stress exerted on a material is related the rate of deformation through viscosity by the following,

$$\sigma = \eta\gamma, \tag{4.1}$$

where σ is stress, η is viscosity, and γ is the rate of deformation.

Viscosity can be measured through the use of a rheometer. By placing the fluid to be measured between two parallel plates and rotating one of the plates, stress is applied to the fluid through torque. This torque creates shearing of the fluid. Varying the rotation speed of the plate allows one to directly control the rate at which shear is applied to the fluid. By

varying this shear rate, we were able to characterize the viscosity of the Ficoll suspensions at shear rates of $100s^{-1}$ to $400s^{-1}$. Achieving shear rates above this was impractical using the rheometer. It should be noted that the expected shear rate experienced by a fluid at the orifice is on the magnitude of $10{,}000s^{-1}$ [100, 101]. The shear thinning behaviour we observed in our experimental results suggests that our measurements are representative of the higher shear rates found in the nozzle. However, viscosity measurements using techniques such as high shear rate viscometry [102] would be valuable for confirmation of this assumption in future work.

4.2.1 Experimental Details

MCF-7 cell suspensions at concentration of 500,000 per mL were prepared in 0% to 15% Ficoll solutions in the same manner as previously described. In addition, solutions containing no cells were also prepared as controls. A Physica MCR-301 rheometer (Anton Parr) was used to characterize viscosities. A ppm25 head (Anton Parr) was used. Briefly, the plate setup was rinsed with 2-isoproponal prior to and in between sample loading. Approximately 400 μL of each sample was used for measurement. The viscosity of each sample was assessed over the course of two minutes, in which twenty individual data points were collected, each 6 seconds apart. Samples were characterized at 4 independent shear rates ($100\ s^{-1}$, $200\ s^{-1}$, $300\ s^{-1}$, $400\ s^{-1}$), in order to assess for the presence of shear-thinning behaviour. All samples were characterized at 25^{0}C.

4.2.2 Results

The inkjet nozzle used in this work is capable of dispensing fluids up to a viscosity of 20 mPa•s. As such, it was important to ensure that any suspension to be dispensed falls within this range. We were interested in neutral buoyancy; the key question was, could we achieve neutral buoyancy within cell suspensions while keeping the viscosity of the suspensions under 20 mPa•s? Neutral buoyancy was achieved at a concentration of approximately 10% Ficoll and the viscosity of this suspension was found to be within the required range. The viscosities of solutions in the absence of cells were also measured. Results are displayed in Figure 4.3. As can be seen, all fluids had a viscosity under the limit of 20 mPa•s.

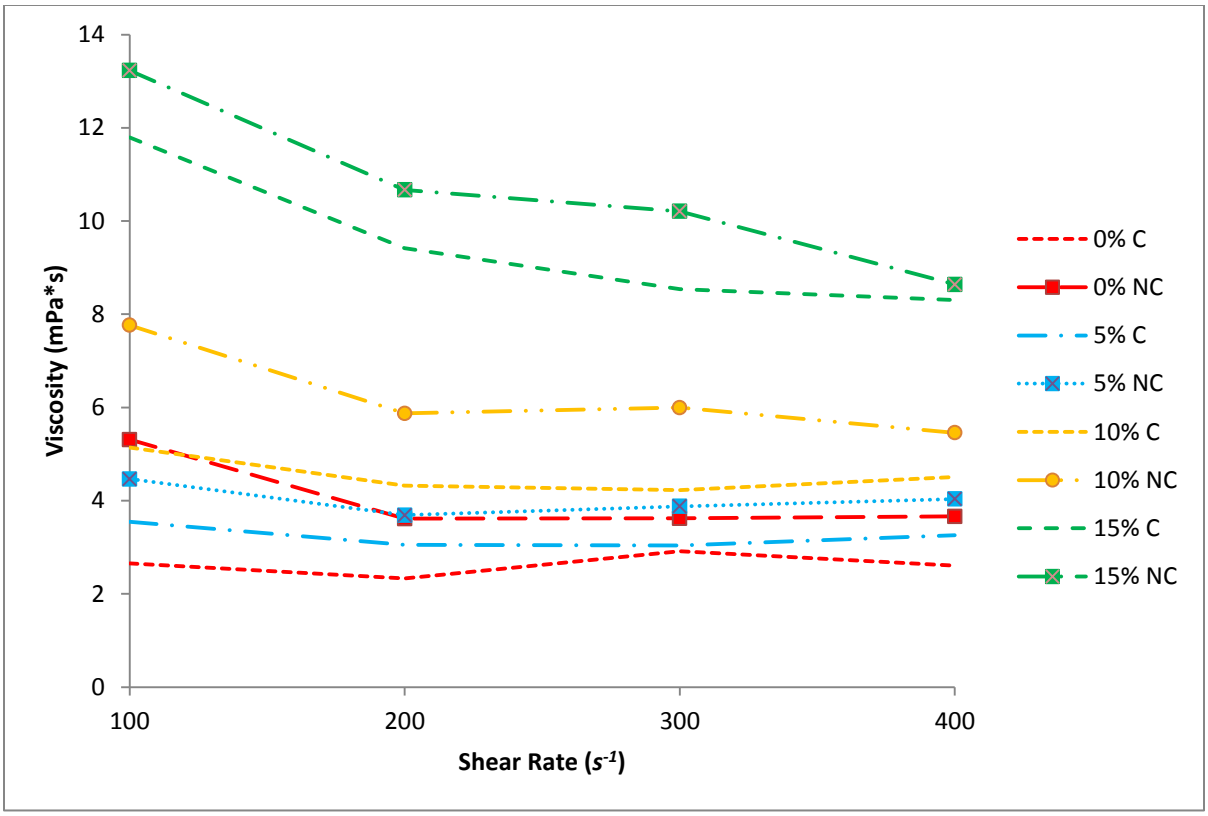

Figure 4.3. Viscosities of cell based (500,000 per mL) Ficoll-PM400 suspensions of 0% to 15%. Ficoll solutions were also assessed without cells. Viscosities were measured at shear rates of $100s^{-1}$ to $400s^{-1}$. All data points seen are averages of 20 measurements at the specified shear rate.

Inkjet printers were originally designed to be used with inks that display specific physical properties [103]. The requirements include appropriate dispersion of solute within solvent to ensure consistency of printing over extended periods of time, low viscosity to ensure sufficient transfer of kinetic energy to the droplet, and finely tuned surface tension that allows for droplet ejection. In this work, we attempted to increase cellular dispersion through the mitigation of cell sedimentation. In addition to raising solution density, Ficoll-PM400 also results in increased viscosity.

Applications such as printed electronics and sensors, and tissue engineering require the dispensing of particle based suspensions as well as polymeric materials. Volume fraction

of particles can influence viscosity as indicated in Chapter 2, and jamming transitions can occur as this fraction reaches particular thresholds. In this work, the volume fraction of cells is low (less than 2%); Derby and co-workers calculated the theoretical volume fraction at which relative viscosity exceeds 20 mPa•s to be between 40% and 45% [69]. Thus, viscosity concerns due to volume fraction were not a concern in this work. Even so, equation 2.3 dictates that the viscosity seen should rise with volume fraction; our results do not agree with this. The suspensions lacking cells displayed higher viscosities than those containing cells. Cells present in solution will actively consume nutrients contained within the culture media solution as well as excrete metabolic waste; this actively changes quantities of molecules found within solution. Presence of cells may alter pH and ionic concentrations within suspensions, which have been shown to alter viscosity [104]. Also, metabolic by products, such as urea, can alter solution viscosity through changes in molecular structure [105]. Cell culture itself is difficult to control and reproduce accurately due to a lack of technologies that can monitor quantities of interest, such as viscosity, in real time [106]. It will be important in future work to consider how cellular presence may alter macroscopic suspension properties.

The high viscosity of polymeric materials, such as Ficoll, results in faster dissipation of waves. This limits the kinetic energy that is transferred to the fluid at the fluid air interface; changes in droplet size are expected [69]. This was an issue seen in this work. Parameter settings on the inkjet printer had to be adjusted for higher viscosity solutions in order to combat these effects. Parameter ranges are detailed in table 4.1. For the cell count analysis found in section 4.4, voltages and pulse lengths were adjusted so that drops of similar size were ejected regardless of Ficoll concentration.

Table 4.1. Parameters used for ejection of cell suspensions containing varying amounts of Ficoll polymer.

Ficoll Concentration (w/v %)	Voltage (V)	Pulse Length (μs)	Frequency of Drop Formation (Hz)
0	60-70	20-23	250
5	70-80	16-21	250
10	80-90	20-23	250

The combination of acoustic resonance properties and impeded kinetic energy has led to what many call the "first drop problem". This phenomenon refers to the fact that the ejection of the first droplet may be impeded until the proper acoustic state within the nozzle is met. Furthermore, even if the droplet is ejected immediately, it will likely not resemble the subsequent droplets in its physical properties [107]. Famili and co-workers revealed a number of phenomena that appear to be driven by differences between the first ejected drop in a burst and those that follow it. The expected linear relationship between driving voltage and drop mass does not hold in these situations. We noticed an exaggerated version of this problem likely due to the increased viscosity of the fluid. Movement of fluid was visible at the orifice, but no drop was ejected. Rather, the first droplet appeared after a few seconds. This suggests that higher viscosity suspensions may cause a decay of waves, and that the proper interaction of waves needed for drop formation is not achieved until later into the process. Regardless, as we mentioned, parameters were adjusted so that the drops being ejected were the same size as those seen when using the 0% and 5% Ficoll suspensions.

In addition to the impact the increased viscosity has on inkjet properties, it also plays a part in the balance of forces experienced by the cells themselves. From equation 2.9, we know that drag increases linearly with viscosity; therefore cells within suspensions containing a higher concentration of Ficoll will experience a greater drag force. Alterations in drag force due to increased velocity profiles has been shown to alter cell separation device function [108], but to our knowledge, manipulation of the fluid viscosity itself has not been explored comprehensively with regards to cellular transport.

4.3 Sedimentation Rates

Solution stability is a key aspect for the reliable function of inkjet printing. Sedimentation of particles within fluid would disturb this stability. Cells are known to sediment in a variety of different contexts, and prior measurements have been accomplished utilizing varied methods. In this study, we utilized digital video microscopy to assess the sedimentation velocities and subsequent density of MCF-7 breast cancer cells in various Ficoll-PM400 solutions.

4.3.1 Characterization Techniques

Cellular sedimentation is a phenomenon that is observed in various engineering and natural science fields. Sedimentation of various cell types is quite common within aqueous terrains and is important for the ecosystem in such areas [109]. Sedimentation is also commonly seen in bioreactor setups [110], and can be used to separate cells from the media [111]. Sedimentation of cells however, can have a negative influence on protein production and collection in bioreactors, and is usually prevented through effective stirring mechanisms [112]. Sedimentation has been hypothesized to hamper performance in inkjet settings; such stirring mechanisms have not been effective [90].

Sedimentation rates can be characterized in various manners, each with their own caveats. Ideally, a direct mass measurement of single cells would allow for calculation of the sedimentation rate using Stokes' Law, however, single cell mass measurements are a very recent technical advance [91] out of the reach of this thesis. Sedimentation rates have also been characterized by simple column setups, where the concentration of cells in particular

chambers is measured over a set length of time [113]. This method is technically simple, but also lacks resolution.

4.3.2 Experimental Details

We utilized a technique known as digital video microscopy [114]. The technique is simple in concept; videos of cells undergoing sedimentation are recorded at various time points and velocities are determined by assessment using a custom MATLAB script. Briefly, cellular suspensions of a concentration of 500,000 cells / mL at varying Ficoll densities were loaded into capillary tubes of 1 mm diameter. The bottoms of the tubes were sealed after loading to prevent leaking of the fluid. The tubes were then illuminated using an LED light source and sedimentation of the cells was recorded using a CMOS monochrome camera (Edmund Optics, EO-1312). The camera recorded videos at 25 frames per second. One minute videos of sedimentation were recorded every 10 minutes over the course of an hour. The focal plane was near the middle of the tube's diameter, reducing influence of wall forces. To reduce any influence further, we only chose cells from the midpoint of the tube within videos for analysis. A depiction of the technique is shown in Figure 4.4.

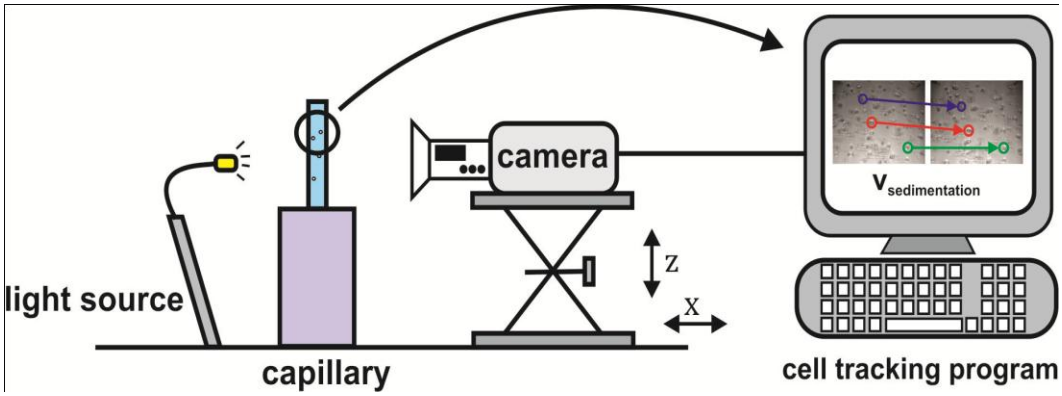

Figure 4.4. A depiction of the experimental set up that was used to capture sedimentation velocities. A light source is used to illuminate a capillary tube that has been filled with a cellular suspension. A camera is used to record videos of the sedimentation at various time points over the course of an hour. A custom particle image velocimetry MATLAB script was used to assess the distance changes that occurred as sedimentation progressed.

4.3.3 Results

The results of the experiment are shown in Figure 4.5. Sedimentation velocities for solutions of 0%, 5%, 10%, and 15% Ficoll were 7.5, 2.3, 0.8, and -0.15 μm/s, respectively. These velocities are from the first time point recorded (at 0 minutes) for each suspension. Neutral buoyancy occurs slightly above 10% Ficoll. A calculation using Stokes' Law reveals a cell density of 1.050 g/mL, very similar to previously reported values [92].

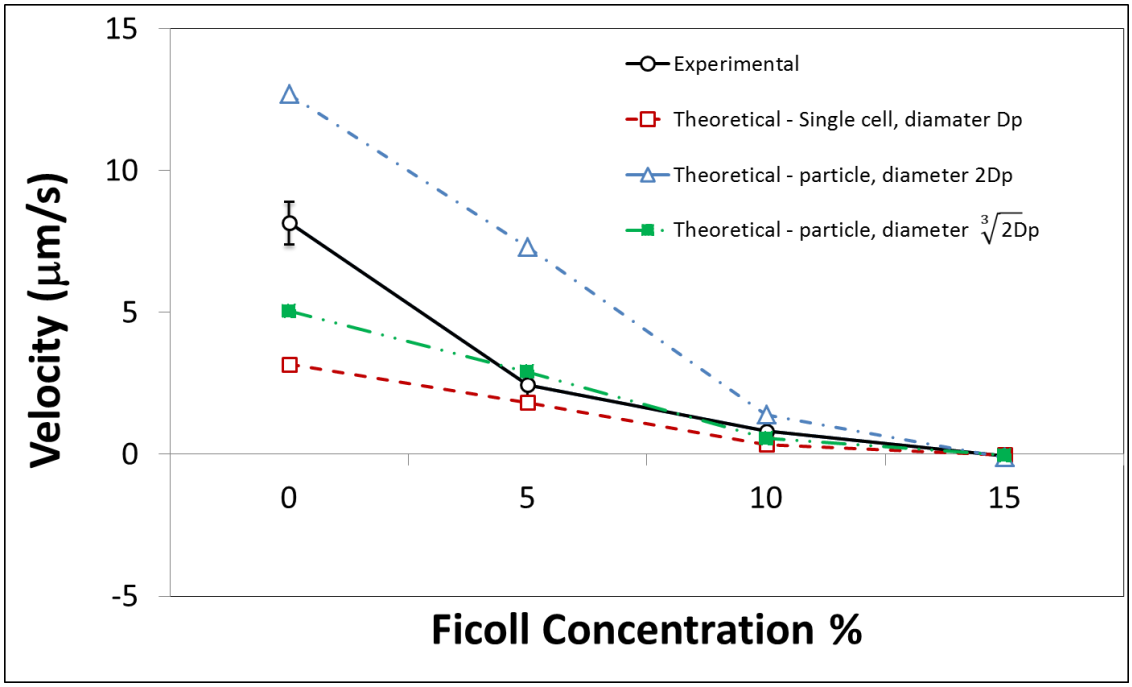

Figure 4.5. Theoretical sedimentation velocities of single cells with diameter $\boldsymbol{D_p}$, a particle which has twice the volume of a single cell (diameter $\boldsymbol{\sqrt[3]{2}D_p}$) and a particle with diameter $\boldsymbol{2D_p}$ (this particle has 8 times the volume of a single cell), as well as the observed experimental velocities. At 0% Ficoll, experimental velocities fall halfway between the single cell and aggregated cells (with diameter $\boldsymbol{2D_p}$) theoretical curves, indicating that a combination of single cells and cell clusters are present; this was confirmed by video analysis.

It is of note that our experimental results fall between the proposed theoretical curves. The 0% suspension in particular shows experimental velocities much greater than those expected for single cells or a pair of cells (diameter $\sqrt[3]{2}D_p$). We believe this is due to the aggregation of cells. From equation 2.10, we know that sedimentation velocity will increase with effective particle diameter. MCF-7 cells are known to aggregate [75], and aggregation of cells has been known to increase sedimentation velocity [109]. At 0% Ficoll, aggregation was observed during video microscopy, as seen in Figure 4.6, and these clusters were seen to sediment faster than single cells. The suspension therefore consisted of both a large number of single cells, as well as cell clusters of varied cell quantities.

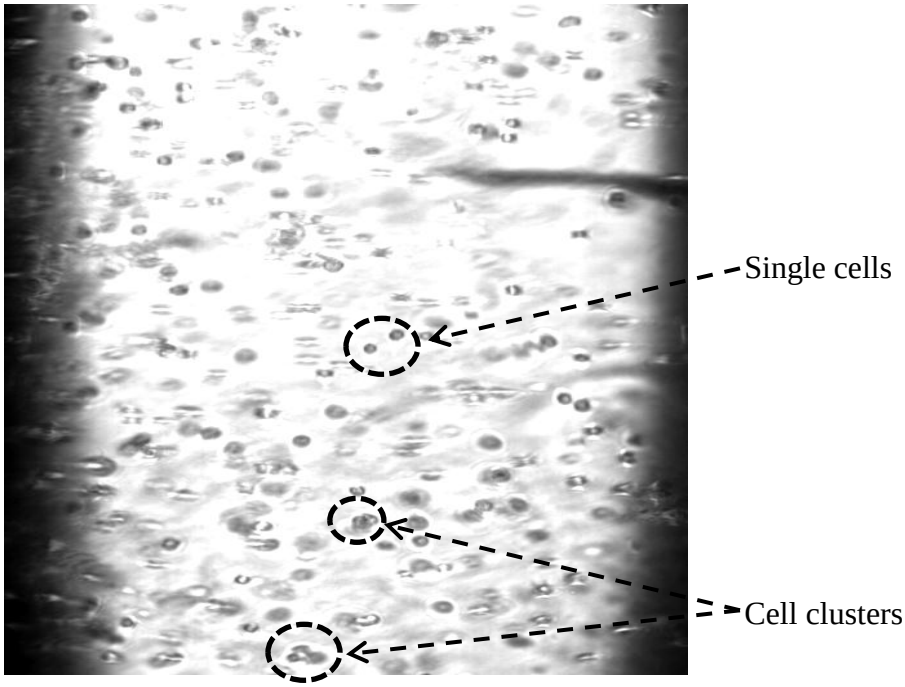

Figure 4.6. A sample image of cellular sedimentation used for velocity determination. This image shows a suspension of cells in the absence of Ficoll polymer. Consecutive images from the same video provided a means to track the same cell as time progressed. From this image, we can see that both single cells and clusters of cells are present.

As density is increased, the difference between the expected sedimentation velocities for different cell clusters decreases. Equation 2.10 again reveals to us the reason for this; values converge due to the decrease in density differences between cells and the surrounding fluid. Although the sedimentation velocities seen for 5% and 10% suspensions are greatly decreased and very similar to what is expected for a single cell, there are still slight differences. This suggests that aggregation of cells may still be occurring at higher density suspensions. The standard deviations in higher density suspensions are also decreased when compared to the 0% suspension, demonstrating that fluctuations in sedimentation velocities due to clusters of different sizes are decreased at these higher densities. From the experimental data, we can extrapolate that neutral buoyancy occurs at a Ficoll concentration slightly above 10%.

4.3.4 Decay in Sedimentation Velocity Over Time

Sedimentation velocities were also charted over a time period of 60 minutes. We can see that there is decay in sedimentation velocity for the 0% solution as time elapses, as shown in Figure 4.7. This is due to the faster sedimentation of larger aggregates at initial time points. The larger aggregated clusters of cells will sediment faster and out of the field of view, leaving the slower sedimenting single cells as seen in Figure 4.8. This effect becomes less pronounced at higher Ficoll concentrations. The standard deviation also decreases as Ficoll concentrations are increased, again demonstrating less variation between the sedimentation velocities of separate cells and aggregates. Overall, this behaviour over time provides evidence that the use of Ficoll based cell suspensions halts sedimentation of cells. Furthermore, the lack of decay seen in the 10% suspension suggests that if aggregation is still occurring in this suspension, these aggregates will not settle out of suspension more quickly than single cells.

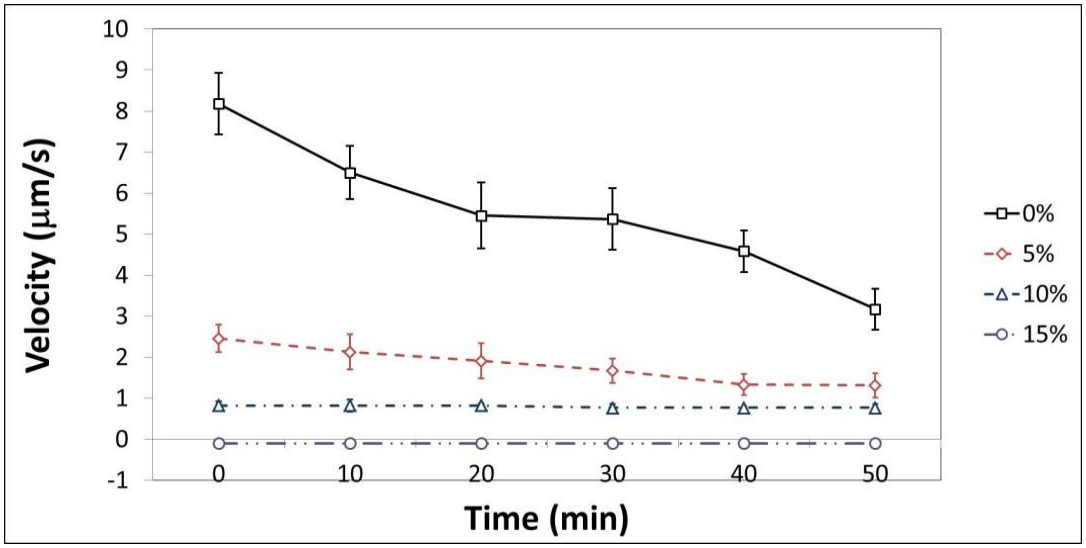

Figure 4.7. Sedimentation velocity at different Ficoll concentrations as a function of time. Large sedimentation velocity decay is observed in the 0% suspension, and slight decay is seen in the 5% suspension.

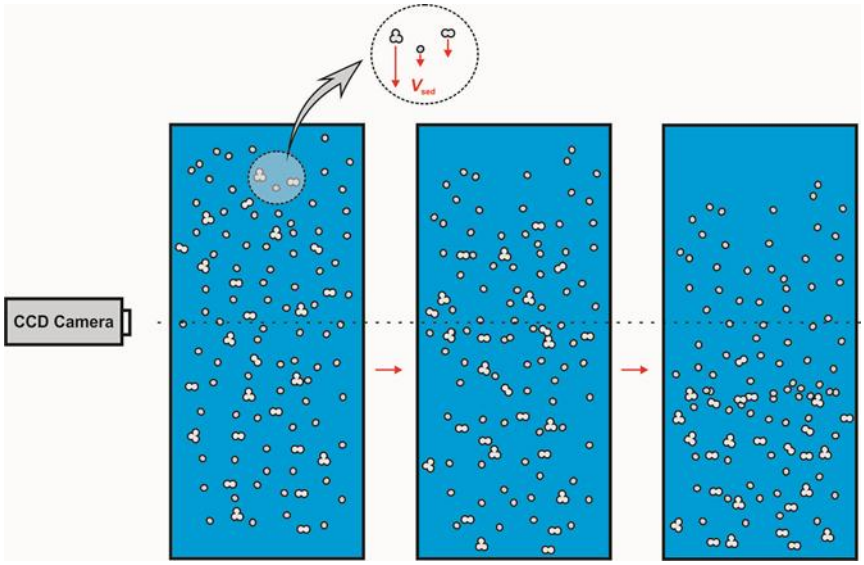

Figure 4.8. The reason for decay in sedimentation velocities. Earlier on, larger clusters will sediment quickly, leaving the only the smaller and slower sedimenting clusters. As such, higher sedimentation velocity measurements will be made at earlier time points and the velocity will decay as time progresses.

Cellular aggregation and sedimentation have been hypothesized to impact the printing behaviour within inkjet systems. Varying cell counts over time [46], large amounts of cells seen in individual droplets [35], and constant clogging occurrences [99] have led to this idea. We have now demonstrated that Ficoll based suspensions can halt cellular sedimentation over extended periods of time. We propose the use of these neutrally buoyant suspensions to ensure consistent printing of cells over long periods of time. This hypothesis is explored in section 4.4.

4.4 Time Lapse Inkjet Reliability Measurements

The promise of inkjet based cellular dispensing depends on its ability to reliably deliver cells over long periods of time. Potential large scale applications such as drug screening and tissue engineering can only be realized if the dispensing and patterning process is reproducible at any given time point. Particularly, the amount of cells being dispensed should stay consistent. Previous reports have hinted that this assumption does not hold true. Large changes in cell counts over time have been seen in many accounts [46, 57]. Sedimentation and aggregation of cells have been proposed as potential causes for these abnormalities, however, a systematic investigation to confirm this hypothesis has not yet been carried out. In this work, we devised a means to systematically investigate the impact sedimentation has on inkjet printer reliability over a time span of 90 minutes. We accomplished this by dispensing a pre-determined number of droplets into separate cell culture wells and then assessing cell count through means of a CyQuant NF DNA binding assay.

4.4.1 Experimental Set Up

The experiment was carried out by programming the inkjet printer to dispense droplets into separate wells of a 96 cell culture plate. The amount of droplets that were dispensed into each well was 30,000. For example, the printer would first dispense 30,000 droplets into well 1, and then dispense 30,000 droplets into well 2, and so on until well 30. In order to see if clogging had occurred during printing, the nozzle was inspected using the stroboscopic camera in between wells. If a clog had occurred, a small stream of fluid was expelled in order to remove the clog and for printing to continue. It should be noted that this

fluid volume can be significant. Although the least amount of fluid possible was ejected, this process may have introduced error into the data set, as we will discuss in section 4.4.3. Each cycle of printing and visualization took 3 minutes, and the time to remove a clog was negligible compared to this. This resulted in a total printing time of 90 minutes. It should be noted that the culture wells were prefilled with 100 μL of DMEM prior to printing to ensure cells did not dry out and that the proper conditions were in place for count readouts (detailed below).

We utilized a cellular concentration of 500,000 per mL for all experiments. Three concentrations of Ficoll were used, 0%, 5%, and 10%. We also measured droplet diameters to be 50 μm, and by calculating the volume of a sphere, we can estimate droplet volume to be 65 pL. A cell count of 975 is expected for each well from the following relation,

$$E = V_d N C, \tag{4.2}$$

where E is the expected cell count per well, V_d is the volume of a droplet, N is the number of droplets ejected, and C is the concentration of the cell suspension. Here, V_d was 65 pL, N was 30,000, and C was 500,000 cells / mL. It should be noted that the error associated with diameter measurements was 5%. This results in an expected error for cell counts of 16%. Accounting for this error, expected cell counts then fall into a range of between 819 and 1,131 for each well.

By separating the printing process into discrete time points, we were able to accomplish a systematic investigation of printing behaviour over time. The amount of cells that were present in each well was compared to the amount of cells that were expected. Furthermore, we were able to track changes in clogging. The experimental setup is displayed in Figure 4.9. The amount of cells in each well was assessed via a CyQuant NF assay.

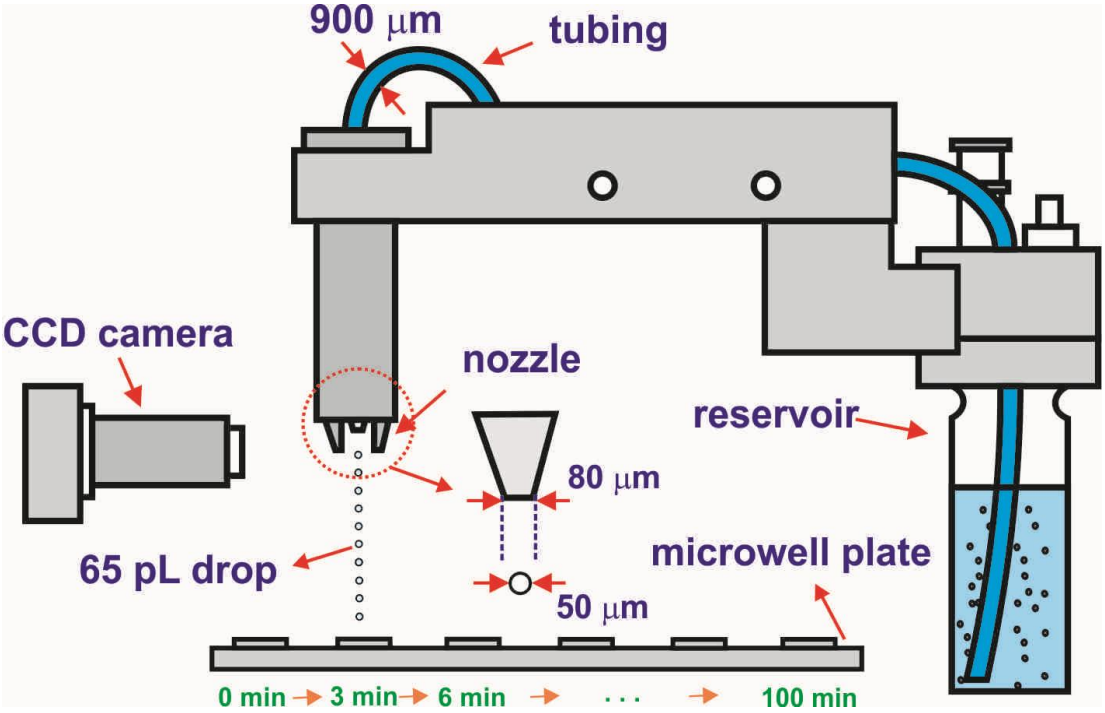

Figure 4.9. The experimental approach that was used for our time lapse analysis. Cells are printed into separate wells over a time span of approximately 100 minutes. It takes 3 minutes to dispense the desired amount of droplets into any given well. A CCD camera was used to image the nozzle between wells to investigate clogging and remove such clogs if necessary.

4.4.2 CyQuant NF Assay

Although cell counting after inkjet printing has been done before, it has mainly been accomplished using MTT or MTS assays, which give the viability of cells after they have attached. There are problems that arise with such an approach. Firstly, these assays are limited to large numbers of cells (at least 10,000), limiting the resolution at which you can track inkjet behaviour. Cell counting has also been done using fluorescence microscopy to observe droplet occupancy [35].

We instead utilized the CyQuant NF assay (Invitrogen) to assess cell count [115]. CyQuant NF assays are based on measurement of cellular DNA content. CyQuant is a highly sensitive cyanine dye that generates large fluorescence once bound to the DNA [116]. The assay gives a good representation of cell number as the amount of DNA per cell is highly regulated. The assay provides a good linear representation of cells in the range from 100 to 20,000. Also, cells do not have to be adherent for this assay to be used. This mitigates any influence cellular proliferation would have on experimental readouts. This assay allowed us to easily track changes to cell counts at a high resolution over time.

After printing was completed, 50 μL of 2X CyQuant buffer (which consisted of CyQuant dye, HBS buffer, and H_2O) was added to each well. Cells were incubated (5% CO_2, 37^0C) for 1 hour and fluorescence was then measured using a DTX880 multimode detector (Beckman Coulter). Measurements of both a standard curve and printed samples were normalized to measurements of control wells containing no cells. Cell counts were determined from these readings.

4.4.3 Results

Experimental results confirmed our hypothesis that neutrally buoyant suspensions would improve the efficiency of inkjet printing. Cell counts over a time span of 90 minutes for Ficoll suspensions of 0%, 5%, and 10% are shown below in Figure 4.10. Each data point in the Figure represents the number of cells ejected at a given time point, and all values are an average of three separate experimental replicates. The error bars represent the standard deviation between the three experimental replicates. The dashed line represents the expected number of cells (975).

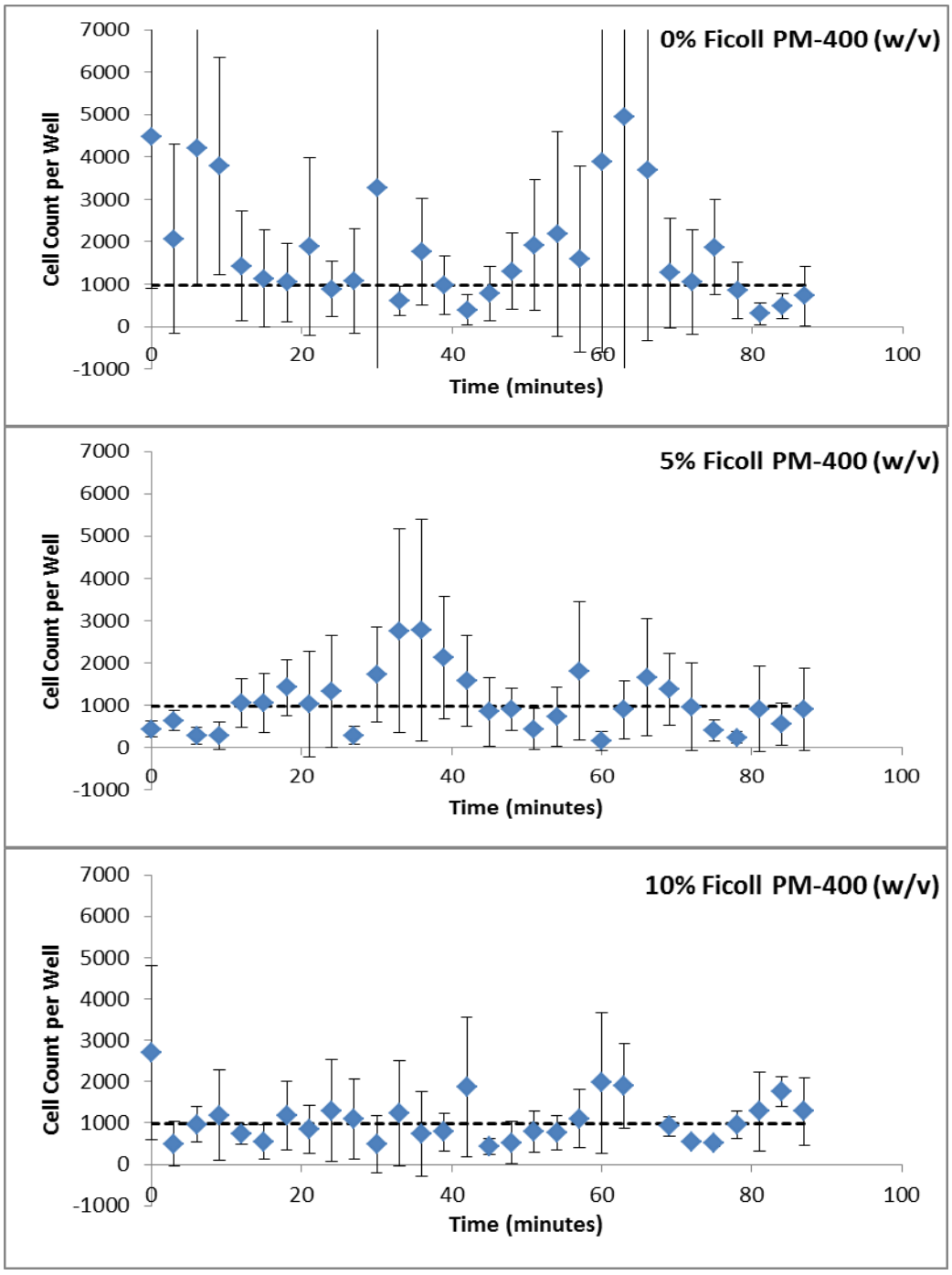

Figure 4.10. Cell count per 30,000 drops, for 0%, 5%, and 10% Ficoll-PM 400 (w/v) cell suspensions (500,000 cells/mL), ejected into subsequent wells over a time of 90 minutes. Dispensing and nozzle inspection took 3 minutes per well, and 30 wells were assessed. Fluctuation of cell count over time and standard deviation are lowest in 10% Ficoll-PM 400 (w/v) suspension. The dashed line represents the expected cell count (975) for droplets of 65 pL volume.

The results demonstrate that the amount of cells being dispensed at a given time point depends on the Ficoll concentration that is used. At 0% Ficoll, large deviations in cell counts, both between replicates and ensuing time points, are seen. Average deviations for this concentration are well over 100%. The average cell count is much greater than the expected value of 975, and even greatly exceeds the upper bound of 1131 cells. The reason for these large counts could be the dispensing of aggregated clusters, or that large amounts of cells may reside at the focal point of ejection due to sedimentation [35]. A trend of decreasing cell count over time due to sedimentation within the reservoir is expected. We do not see such a trend, which could be due to the high occurrence of clogging during the printing process when using this suspension. As we mentioned, fluid had to be ejected in order to remove these clogs. Although we attempted to eject the least amount of fluid possible to remove clogs, the frequent ejection may have led to a large amount of the suspension being manually dispensed. This may have re-suspended cells within the reservoir, or caused deviations of cell concentration that may help to explain the large irregularity of cell counts. Regardless, printing this suspension proved to be difficult, inefficient, and yielded no signs of accuracy or reliability.

The Ficoll stabilized solutions both showed a greater consistency of printing over time. Average cell counts for these two suspensions were almost identical and very close to the expected value of 975. Deviations from the expected count over time points were drastically reduced when compared to the control suspension (from 101% to 41%). Nozzle clogging was completely eliminated, and the frequency of both negligible and high cell counts was reduced. The 10% suspension, where neutral buoyancy is almost achieved, displayed the greatest improvement in performance. The level of accuracy and the reliability

over time achieved with the manipulated cell suspensions immediately highlight the potential of the approach.

Although the average deviation from the expected value was significantly reduced, values are still large (54% and 41%). However, these deviations are based on the exact value of 975 cells per well and it was noted that an expected error of 16% due to imaging exists as described in section 4.4.1. Accounting for this error, we can establish both minimum and maximum values of expected cell count. Additionally, we can establish a lower bound and upper bound for cell counts at each Ficoll concentration by accounting for the deviation seen and the average expected count of 975. This allows us to visualize how the range of observed cell counts varies from the expected range, as seen in Figure 4.11. From this, it is apparent that the range of observed cell counts decreases with increasing Ficoll concentration. Even at 10% however, the range of observed cell counts is larger than expected, even when accounting for imaging error. At a cell concentration of 500,000 cells / mL it would take 30 droplets of 65 pL volume (the size produced in these experiments) to theoretically dispense one cell. At such low volume fractions, minor stratifications of concentration within the fluid could cause large deviations in cell count. Precision could be increased by raising cell concentration; however, an upper limit on concentration is dictated by nozzle clogging. It should also be noted that a large amount of wells with a cell count of 0 or greater than 3000 were detected when using the 0% suspension. The incidence of these events was decreased when using the Ficoll stabilized suspensions. As mentioned, the CyQuant assay gives a good representation of cells between counts of 100 to 20,000. If the cell count within a well was less than 100, it may have been recorded as a well containing no cells. In future work we will

further verify cell counts fewer than 100 using other means such as fluorescence microscopy. The total results of these experiments are summarized in Table 4.2.

This work shows that density balancing is a viable approach to increasing inkjet dispensing consistency and reliability. Density balancing has been used in microfluidic devices before [117, 118], but has not been applied to inkjet printing. Furthermore, the materials used in these microfluidic applications were glycerol and alginate; the viscosity of both these materials is much too great to be used in inkjet printing.

The fact that nozzle clogging is reduced when Ficoll concentration is increased is likely due to a complex balance of forces. Changes in density and viscosity affect flow behaviour, drag forces, sedimentation, and deposition behaviours. Characterization of how these changes impact particle trajectories will be important for further development of such systems.

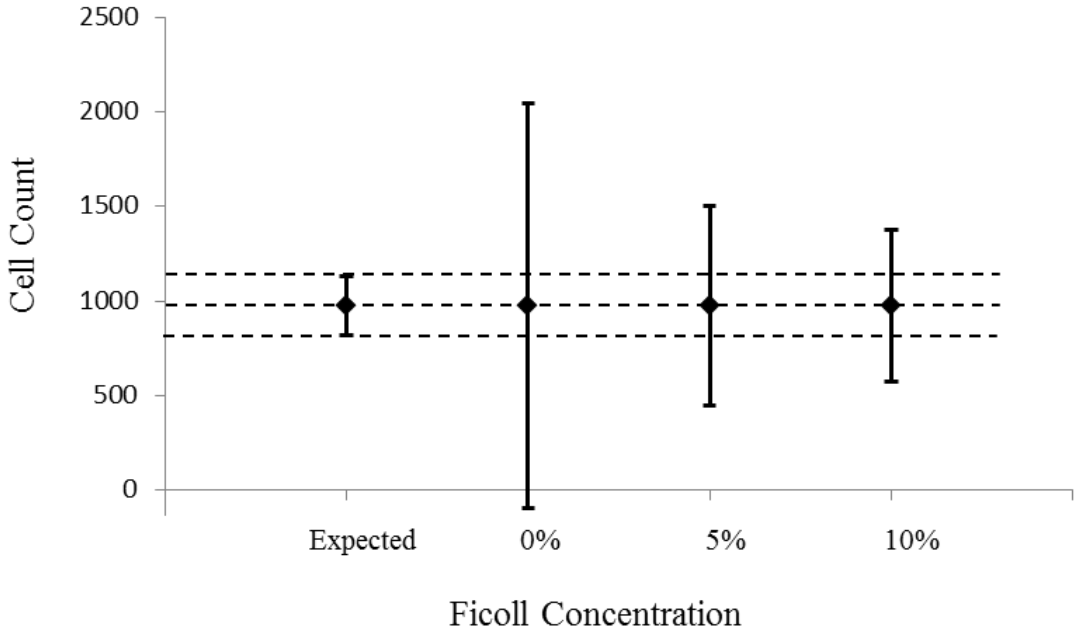

Figure 4.11. The range of observed cell counts as a function of Ficoll concentration. The dashed lines represent the average (975), minimum (819) and maximum (1131) cell counts expected based on droplet volume calculations and accounting for imaging error. The error bars depict the average deviation seen for cell counts at particular Ficoll concentrations compared to the expected value of 975. From this graph, we can see that deviation decreases as a function of Ficoll concentration. The range of observed counts for a suspension of 10% Ficoll is closest to the expected range.

Table 4.2. Average counts and deviation from expected for the three cell suspensions, over the course of 90 minutes. Values are calculated from all thirty cell counts collected throughout experiments shown in Figure 4.10. Values used for calculations are themselves averages from three experimental replicates. Frequency of nozzle failure, average time to clogging +/- standard deviation, frequency of negligible cell counts (fluorescence values displaying no difference from control wells), and frequency of very high cell counts (3000+), are also shown.

Sample (% Ficoll)	Average number of cells per well	Expected cells per well	Average Deviation from expected (975) (%)	Minimum expected cells (Expected - error)	Maximum expected cells (Expected + error)
0%	1859	975	110%	819	1131
5%	1052	975	54%	819	1131
10%	1066	975	41%	819	1131

Lower bound cell count (Expected – deviation)	Upper bound cell count (Expected + deviation)	Frequency of Nozzle Failure	Average Time to Clogging (+/- St. Dev.) (minutes)	0 Cells per well	>3000 Cells per well
0	2047	23%	8 (+/- 7)	8.7%	18.75%
449	1501	--	--	3.3%	10.7%
575	1375	--	--	3.1%	7.1%

Chapter 5: Conclusion and Future Work

5.1 Summary of the Results

Cellular sedimentation, aggregation, and deposition all interfere with the performance of the inkjet system. Such effects must be addressed in order to fully realize the potential of inkjet dispensing for biological applications. In this study we focused solely on halting sedimentation of cells through changes in fluid density. We attempted to create neutrally buoyant cell suspensions that did not alter cell viability, but improved the inkjet dispensing process. Ficoll-PM400 is a sucrose copolymer commonly used in cell separation applications which has been validated for many other cell based purposes. Ficoll raises both density and viscosity of solutions. In relation to other density altering compounds, Ficoll's effect on viscosity is much less. We utilized digital video microscopy to assess the concentration of Ficoll at which cells achieved neutral buoyancy. We also characterized the viscosity of these cell based suspensions and found that they stayed under the 20 mPa•s threshold that is allowed by our piezoelectric inkjet system.

The effect of suspension stabilization on inkjet printing reliability was measured using a time-lapse dispensing experiment. The piezoelectric system was automated to eject a pre-determined amount of drops into separate compartments over a period of 90 minutes. Cell counts were then assessed using a DNA binding assay known as CyQuant NF. We found dispensing reliability improved significantly as suspensions reached neutral buoyancy. Suspensions that were prepared in the absence of Ficoll resulted in poor inkjet performance over the course of the experiment. It was found that out of the three Ficoll based suspensions

of concentrations 0%, 5%, and 10%, a suspension of 10% Ficoll generated the best results. Additionally, the occurrence of nozzle clogging was significantly reduced with the addition of Ficoll under controlled experimental parameters. Clogging was quite frequent in the absence of Ficoll (occurrence approximately every 8 minutes), and was negligible when using Ficoll based suspensions.

Although the initial focus of this study was to use increases in solution density to halt sedimentation and improve inkjet performance, the changes in viscosity also had incidental effects on the process although these effects have yet to be precisely characterized. In particular, the increased viscosities of Ficoll based cell suspensions resulted in different operating parameters, likely due to acoustic damping, as well decreased clogging events which may be due to increased drag forces within the system.

5.2 Future Work

This thesis has outlined a method for the repeatable and reliable dispensing of cellular suspensions using density balancing through the sucrose copolymer, Ficoll-PM400. However, there is still large room for improvement and investigation of this process. Suspensions could be optimized and cell interaction phenomena could be investigated, the dynamics and physical nature of particle encapsulation and clogging should be investigated, the printing process could be optimized and substrate dynamics be considered, and applications should now be envisioned.

5.2.1 Cellular Aggregation Considerations and Optimization

This work focused on mitigating sedimentation of cells within a suspension intended for use with inkjet printing. This simple optimization showed dramatic increase in technical performance. However, there are likely numerous other phenomena within such suspensions that should be accounted for and investigated.

Cellular aggregation is the first concern. Aggregation was documented during the printing process, and the deviation of experimental sedimentation velocities from those that are expected for a single cell suggests that aggregation may still be a considerable factor even when using high Ficoll concentration suspensions. Aggregation of cells may cause physical blockages of channels, and will result in uneven dispensing. Aggregation is a function of particular adhesion molecules located on the surface membranes of the cells. Cadherin and integrin proteins have distinct functional roles in creating strong cell to cell adhesions. The relative abundance of these proteins is dependent on the cell type under question. As such, not all cells will display significant aggregation behaviour. For those cells that do, understanding the dynamics of aggregation under experimental situations of interest is still a poorly defined field.

The parameters influencing aggregation may be quite diverse. From a molecular standpoint, integrin and cadherin proteins will functionally depend on the physicochemical environment. For example, cadherins are dependent on the presence of calcium ions [73]. Concentration dependent effects could alter structure and behaviour of the proteins. In addition, the presence of other enzymes could have a profound impact on behaviour of these enzymes through functional activation. Fluid flow, shear stress, and pressure can all influence the manner in which such cellular molecules interact [119, 120]. From a cellular

and physical standpoint, aggregation is likely dependent on the composition of the environment and the rate of inter particle interactions. For example, cell to cell interactions and changes in flow orientation during red blood cell flow have been observed to be dependent on capillary diameter; these effects become less pronounced as diameter decreases [121]. Additionally, both cell velocity and interaction time have been implicated in whether or not cell adhesion occurs during flow for a variety of different cell types [122].

New technologies allow for further assessment of such parameters. For example, microfluidic devices are now being used to investigate how parameters such as shear can contribute to cellular aggregation events [123]. Insights gathered from these types of studies will have relevance to cell suspension applications. Suspension additives such as salt ions or antibodies may help reduce this behaviour when needed. Optimization of fluid additives is needed for improving inkjet dispensing reliability further, and optimization for different cell types as well as co-suspensions (multiple cell types in same suspension) is needed. We suggest this is an important area that should be interrogated through the use of relevant technologies. For example, microfluidic devices that mimic features of an inkjet system could be used to quickly and quantitatively assess the impact of additives on cellular aggregation. Experiments using varied quantities of antibodies targeted toward adhesion molecules could also be used to explore the extent of aggregation when using higher Ficoll concentration suspensions.

5.2.2 Physical Understanding and Optimization of Printing Events

This work attempted to quantify the effects of sedimentation on inkjet reliability over a set period of dispensing time. Our approach focused on changing solution density, which

also resulted in a change in viscosity. Although our analysis of sedimentation yielded positive results, we also witnessed several incidental phenomena that are likely related to the changes in viscosity. It will be important to understand precisely why these events occurred in order to effectively implement inkjet technology for cell dispensing applications in the future.

The first event of interest was the clogging that was witnessed at the nozzle orifice as well as the reduction of this clogging as Ficoll concentration was increased. We witnessed that even at a low volume fraction, in the absence of Ficoll cells would adhere to walls and re-circulate at locations near the nozzle opening, and remain there while fluid was still being dispensed. Re-circulation of cells near the focal point where a droplet ejects has been observed previously, although for an ejection method that does not make use of a nozzle [35]. Furthermore, for our experiments, this buildup of cells near the orifice would continue over time until full blockage of the opening occurred, effectively halting droplet generation. Particles are known to migrate from regions of high shear to low shear, and shear induced forces have been implicated in the re-suspension of settled particles [124]. It is possible that the large amount of shear generated near the orifice prevents a proportion of cells from being ejected. When Ficoll was added to suspension, the amount of cells that would adhere to and re-circulate around this area was reduced. Furthermore, we also witnessed that large aggregates (larger than the orifice opening) would be dispensed, even if they halted temporarily at the opening. Stokes' Law indicates that drag increases with viscosity; this increased drag may overcome the shear present at the orifice and enable effective cell dispensing. However, this has not yet been clearly demonstrated. It would be valuable to assess this phenomenon through the use of a technique such as particle image velocimetry

(PIV). If promising explanations are revealed, investigation of the influence of system parameters on this phenomenon would also be useful.

Secondly, we noted that suspensions of increased viscosity required higher voltages for droplet ejection. Viscosity results in higher rates of wave attenuation; in other words, a wave generated by piezoelectric actuation will decay faster in a solution of higher viscosity [68]. We have noted that proper droplet ejection depends on appropriate wave interactions and the sufficient transfer of kinetic energy to the fluid air interface. In the highest viscosity suspension, droplets began to eject a few seconds after actuation was begun. This suggests that enough energy was transferred to the interface eventually, but that the energy of the initial waves itself was not sufficient as these waves decayed too quickly to generate the appropriate wave amplification. Acoustic attenuation within dilute suspensions of particles is also a topic of interest being explored by other groups, and may prove to be relevant for this application [125]. Further exploration of the acoustic phenomena within inkjet nozzles being utilized to eject viscous particle suspensions would be useful to determine appropriate operating parameters.

Lastly, although not investigated in this work, the interaction of ejected liquid with substrate of choice should be investigated. The manner in which the liquid impacts the substrate will dictate the feature resolution and fidelity. These parameters are important for various applications. Addition of polymers, such as Ficoll, to the solution will change the manner in which such deposition occurs [126]. In order to effectively predict the consequence of using such materials for cell based inkjet dispensing, this particular phenomenon should be extensively characterized. Both the fluid and substrate could be modified in order to achieve a particular patterning goal. The goal in mind will likely depend

on the application at hand. For example, whereas a cellular microarray may require high density patterns with fine resolution, a larger tissue engineered construct will likely not require such precise control.

5.3 Applications

The application of neutral buoyancy in small volume cell handling systems encompasses many areas of the medical sciences. This method immediately allows for the implementation of inkjet technologies for cell based assays. Drug development pipelines will benefit from the ability to precisely manipulate cell quantities and perform much higher levels of multiplexed assays. The benefit of cost savings is apparent by reducing the volume used per assay. Not as obvious, however, is the increased information output such multiplexed assays could provide. Multiple drug combinations, concentrations, as well as combination with gene knockout reagents, could enable vast amounts of quantitative cell signalling network information to be gathered rapidly [127]. Most drugs target one particular component of a signalling pathway; data is usually not gathered for off target effects due to biological unknowns [128]. Multiplexing assays through dispensing inkjet technologies would enable such off target effects to be assessed early on into the process, and provide a greater overall understanding of the impact that a particular drug would have on cellular targets.

Another application is the creation of cellular microarrays [6]. Such arrays, which can be thought of as very high density cell cultures plates, could be useful for both drug development and basic research. DNA microarrays have gained vast adoption throughout the biomedical arena due to their ability to cheaply and reliably provide multiplexed genetic

information on biological samples. Such arrays, however, only provide fixed time point readouts and do not give information regarding function of particular genetic components. Creation of living cell microarrays could allow for functional assessment of genes through combination with siRNA methodologies. The simple miniaturization of cell based assays through such a format could allow for basic researchers to generate data more quickly and effectively, providing an overall increase in productivity of this sector of research.

The last application deals with the disruptive research opportunities such technology allows. The first deals with micro positioning of cells. The rapid dispensing allowed by inkjet technologies could allow for rapid creation of particular cell patterns which could then be quantitatively assessed for function based on structure. Such positional cues are beginning to be recognized as important factors in areas such as development, organ function, and cancer [129]. Furthermore, inkjet technology can be extended from this paradigm into the field of tissue engineering. By effectively allowing proper dispensing of cells, these cells could be arranged in the manner necessary for the creation of functional tissue replacement composites [130].

Bibliography

1. Hertzberg, R.P. and A.J. Pope, *High-throughput screening: new technology for the 21st century.* Curr Opin Chem Biol, 2000. **4**(4): p. 445-51.
2. Hansen, C. and S.R. Quake, *Microfluidics in structural biology: smaller, faster em leader better.* Curr Opin Struct Biol, 2003. **13**(5): p. 538-44.
3. Gribbon, P., R. Lyons, P. Laflin, J. Bradley, C. Chambers, B.S. Williams, W. Keighley, and A. Sewing, *Evaluating real-life high-throughput screening data.* J Biomol Screen, 2005. **10**(2): p. 99-107.
4. Malo, N., J.A. Hanley, S. Cerquozzi, J. Pelletier, and R. Nadon, *Statistical practice in high-throughput screening data analysis.* Nat Biotechnol, 2006. **24**(2): p. 167-75.
5. Osorio, N., *Statistics on the table: On the history of statistical concepts and methods.* Library Journal, 1999. **124**(17): p. 102-102.
6. Fernandes, T.G., M.M. Diogo, D.S. Clark, J.S. Dordick, and J.M. Cabral, *High-throughput cellular microarray platforms: applications in drug discovery, toxicology and stem cell research.* Trends Biotechnol, 2009. **27**(6): p. 342-9.
7. Kunkel, E.J., *Systems biology in drug discovery.* Conf Proc IEEE Eng Med Biol Soc, 2006. **1**: p. 37.
8. Beske, O.E. and S. Goldbard, *High-throughput cell analysis using multiplexed array technologies.* Drug Discovery Today, 2002. **7**(18): p. S131-S135.
9. Jakab, K., C. Norotte, F. Marga, K. Murphy, G. Vunjak-Novakovic, and G. Forgacs, *Tissue engineering by self-assembly and bio-printing of living cells.* Biofabrication, 2010. **2**(2): p. 022001.
10. Ingber, D.E., *Cellular basis of mechanotransduction.* Biol Bull, 1998. **194**(3): p. 323-5; discussion 325-7.
11. Huh, D., Y.S. Torisawa, G.A. Hamilton, H.J. Kim, and D.E. Ingber, *Microengineered physiological biomimicry: Organs-on-Chips.* Lab Chip, 2012. **12**: p. 2156-64.
12. Thery, M., *Micropatterning as a tool to decipher cell morphogenesis and functions.* Journal of Cell Science, 2010. **123**(24): p. 4201-4213.
13. Kenny, P.A., G.Y. Lee, and M.J. Bissell, *Targeting the tumor microenvironment.* Front Biosci, 2007. **12**: p. 3468-74.
14. Hierlemann, A., O. Brand, C. Hagleitner, and H. Baltes, *Microfabrication techniques for chemical/biosensors.* Proceedings of the Ieee, 2003. **91**(6): p. 839-863.
15. Grayson, A.C.R., R.S. Shawgo, A.M. Johnson, N.T. Flynn, Y.W. Li, M.J. Cima, and R. Langer, *A BioMEMS review: MEMS technology for physiologically integrated devices.* Proceedings of the Ieee, 2004. **92**(1): p. 6-21.
16. Whitesides, G.M., E. Ostuni, S. Takayama, X. Jiang, and D.E. Ingber, *Soft lithography in biology and biochemistry.* Annu Rev Biomed Eng, 2001. **3**: p. 335-73.
17. Yu, L., H. Huang, X. Dong, D. Wu, J. Qin, and B. Lin, *Simple, fast and high-throughput single-cell analysis on PDMS microfluidic chips.* Electrophoresis, 2008. **29**(24): p. 5055-60.
18. Khetani, S.R. and S.N. Bhatia, *Microscale culture of human liver cells for drug development.* Nat Biotechnol, 2008. **26**(1): p. 120-6.

19. Pla-Roca, M., J.G. Fernandez, C.A. Mills, E. Martinez, and J. Samitier, *Micro/nanopatterning of proteins via contact printing using high aspect ratio PMMA stamps and nanoimprint apparatus.* Langmuir, 2007. **23**(16): p. 8614-8.
20. Wang, Y., Z. Chen, L. Xiao, Z. Du, X. Han, X. Yu, and Y. Lu, *Evaluating cell migration in vitro by the method based on cell patterning within microfluidic channels.* Electrophoresis, 2012. **33**(5): p. 773-9.
21. Allazetta, S., S. Cosson, and M.P. Lutolf, *Programmable microfluidic patterning of protein gradients on hydrogels.* Chem Commun (Camb), 2011. **47**(1): p. 191-3.
22. Gillette, B.M., J.A. Jensen, B. Tang, G.J. Yang, A. Bazargan-Lari, M. Zhong, and S.K. Sia, *In situ collagen assembly for integrating microfabricated three-dimensional cell-seeded matrices.* Nat Mater, 2008. **7**(8): p. 636-40.
23. Piner, R.D., J. Zhu, F. Xu, S. Hong, and C.A. Mirkin, *"Dip-Pen" nanolithography.* Science, 1999. **283**(5402): p. 661-3.
24. Lee, K.B., S.J. Park, C.A. Mirkin, J.C. Smith, and M. Mrksich, *Protein nanoarrays generated by dip-pen nanolithography.* Science, 2002. **295**(5560): p. 1702-5.
25. Sekula, S., J. Fuchs, S. Weg-Remers, P. Nagel, S. Schuppler, J. Fragala, N. Theilacker, M. Franzreb, C. Wingren, P. Ellmark, C.A. Borrebaeck, C.A. Mirkin, H. Fuchs, and S. Lenhert, *Multiplexed lipid dip-pen nanolithography on subcellular scales for the templating of functional proteins and cell culture.* Small, 2008. **4**(10): p. 1785-93.
26. Wang, C., G. Meng, L. Zhang, Z. Xiong, and J. Liu, *Physical properties and biocompatibility of a core-sheath structure composite scaffold for bone tissue engineering in vitro.* J Biomed Biotechnol, 2012. **2012**: p. 579141.
27. Jakab, K., A. Neagu, V. Mironov, R.R. Markwald, and G. Forgacs, *Engineering biological structures of prescribed shape using self-assembling multicellular systems.* Proc Natl Acad Sci U S A, 2004. **101**(9): p. 2864-9.
28. Marga, F., A. Neagu, I. Kosztin, and G. Forgacs, *Developmental biology and tissue engineering.* Birth Defects Res C Embryo Today, 2007. **81**(4): p. 320-8.
29. Xu, F., J. Celli, I. Rizvi, S. Moon, T. Hasan, and U. Demirci, *A three-dimensional in vitro ovarian cancer coculture model using a high-throughput cell patterning platform.* Biotechnol J, 2011. **6**(2): p. 204-12.
30. Mironov, V., R.P. Visconti, V. Kasyanov, G. Forgacs, C.J. Drake, and R.R. Markwald, *Organ printing: tissue spheroids as building blocks.* Biomaterials, 2009. **30**(12): p. 2164-74.
31. Levenberg, S., J. Rouwkema, M. Macdonald, E.S. Garfein, D.S. Kohane, D.C. Darland, R. Marini, C.A. van Blitterswijk, R.C. Mulligan, P.A. D'Amore, and R. Langer, *Engineering vascularized skeletal muscle tissue.* Nat Biotechnol, 2005. **23**(7): p. 879-84.
32. Pataky, K., T. Braschler, A. Negro, P. Renaud, M.P. Lutolf, and J. Brugger, *Microdrop Printing of Hydrogel Bioinks into 3D Tissue-Like Geometries.* Adv Mater, 2011. **24**(3): p. 391-396.
33. Guillemot, F., A. Souquet, S. Catros, and B. Guillotin, *Laser-assisted cell printing: principle, physical parameters versus cell fate and perspectives in tissue engineering.* Nanomedicine (Lond), 2010. **5**(3): p. 507-15.
34. Guillemot, F., A. Souquet, S. Catros, B. Guillotin, J. Lopez, M. Faucon, B. Pippenger, R. Bareille, M. Remy, S. Bellance, P. Chabassier, J.C. Fricain, and J. Amedee, *High-*

throughput laser printing of cells and biomaterials for tissue engineering. Acta Biomater, 2010. **6**(7): p. 2494-500.
35. Demirci, U. and G. Montesano, *Single cell epitaxy by acoustic picolitre droplets.* Lab Chip, 2007. **7**(9): p. 1139-45.
36. Klebe, R.J., *Cytoscribing: a method for micropositioning cells and the construction of two- and three-dimensional synthetic tissues.* Exp Cell Res, 1988. **179**(2): p. 362-73.
37. Roth, E.A., T. Xu, M. Das, C. Gregory, J.J. Hickman, and T. Boland, *Inkjet printing for high-throughput cell patterning.* Biomaterials, 2004. **25**(17): p. 3707-15.
38. Xu, T., J. Jin, C. Gregory, J.J. Hickman, and T. Boland, *Inkjet printing of viable mammalian cells.* Biomaterials, 2005. **26**(1): p. 93-9.
39. Derby, B.M., B.J. Wilhelmi, E.G. Zook, and M.W. Neumeister, *Flexor tendon reconstruction.* Clin Plast Surg, 2011. **38**(4): p. 607-19.
40. Xu, T., J. Rohozinski, W. Zhao, E.C. Moorefield, A. Atala, and J.J. Yoo, *Inkjet-mediated gene transfection into living cells combined with targeted delivery.* Tissue Eng Part A, 2009. **15**(1): p. 95-101.
41. Goldmann, T. and J.S. Gonzalez, *DNA-printing: utilization of a standard inkjet printer for the transfer of nucleic acids to solid supports.* J Biochem Biophys Methods, 2000. **42**(3): p. 105-10.
42. Arrabito, G. and B. Pignataro, *Inkjet printing methodologies for drug screening.* Anal Chem, 2010. **82**(8): p. 3104-7.
43. Xu, T., C.A. Gregory, P. Molnar, X. Cui, S. Jalota, S.B. Bhaduri, and T. Boland, *Viability and electrophysiology of neural cell structures generated by the inkjet printing method.* Biomaterials, 2006. **27**(19): p. 3580-8.
44. Yamazoe, H. and T. Tanabe, *Cell micropatterning on an albumin-based substrate using an inkjet printing technique.* J Biomed Mater Res A, 2009. **91**(4): p. 1202-9.
45. Siegel, D.M., *Inkjet cell fabricator prints out healing flesh directly onto wounds.* Ostomy Wound Manage, 2010. **56**(4): p. following 85.
46. Saunders, R.E., J.E. Gough, and B. Derby, *Delivery of human fibroblast cells by piezoelectric drop-on-demand inkjet printing.* Biomaterials, 2008. **29**(2): p. 193-203.
47. Cui, X., D. Dean, Z.M. Ruggeri, and T. Boland, *Cell damage evaluation of thermal inkjet printed Chinese hamster ovary cells.* Biotechnol Bioeng, 2010. **106**(6): p. 963-9.
48. Derby, B., *Bioprinting: inkjet printing proteins and hybrid cell-containing materials and structures.* Journal of Materials Chemistry, 2008. **18**(47): p. 5717-21.
49. Cui, X. and T. Boland, *Human microvasculature fabrication using thermal inkjet printing technology.* Biomaterials, 2009. **30**(31): p. 6221-7.
50. Phillippi, J.A., E. Miller, L. Weiss, J. Huard, A. Waggoner, and P. Campbell, *Microenvironments engineered by inkjet bioprinting spatially direct adult stem cells toward muscle- and bone-like subpopulations.* Stem Cells, 2008. **26**(1): p. 127-34.
51. Merrin, J., S. Leibler, and J.S. Chuang, *Printing multistrain bacterial patterns with a piezoelectric inkjet printer.* PLoS One, 2007. **2**(7): p. e663.
52. Choi, W.S., D. Ha, S. Park, and T. Kim, *Synthetic multicellular cell-to-cell communication in inkjet printed bacterial cell systems.* Biomaterials, 2011. **32**(10): p. 2500-7.

53. Xu, T., H. Kincaid, A. Atala, and J.J. Yoo, *High-Throughput Production of Single-Cell Microparticles Using an Inkjet Printing Technology.* Journal of Manufacturing Science and Engineering, 2008. **130**(2): p. 021017.
54. Rose, D., *Microdispensing technologies in drug discovery.* Drug Discov Today, 1999. **4**(9): p. 411-419.
55. Nishiyama, Y., M. Nakamura, C. Henmi, K. Yamaguchi, S. Mochizuki, H. Nakagawa, and K. Takiura, *Development of a three-dimensional bioprinter: construction of cell supporting structures using hydrogel and state-of-the-art inkjet technology.* J Biomech Eng, 2009. **131**(3): p. 035001.
56. Ilkhanizadeh, S., A.I. Teixeira, and O. Hermanson, *Inkjet printing of macromolecules on hydrogels to steer neural stem cell differentiation.* Biomaterials, 2007. **28**(27): p. 3936-43.
57. Hsieh, H.B., J. Fitch, D. White, F. Torres, J. Roy, R. Matusiak, B. Krivacic, B. Kowalski, R. Bruce, and S. Elrod, *Ultra-high-throughput microarray generation and liquid dispensing using multiple disposable piezoelectric ejectors.* J Biomol Screen, 2004. **9**(2): p. 85-94.
58. Parzel, C.A., M.E. Pepper, T. Burg, R.E. Groff, and K.J. Burg, *EDTA enhances high-throughput two-dimensional bioprinting by inhibiting salt scaling and cell aggregation at the nozzle surface.* J Tissue Eng Regen Med, 2009. **3**(4): p. 260-8.
59. Pepper, M.E., V. Seshadri, T.C. Burg, K.J. Burg, and R.E. Groff, *Characterizing the effects of cell settling on bioprinter output.* Biofabrication, 2012. **4**(1): p. 011001.
60. Martin, G.D., S.D. Hoath, and I.M. Hutchings, *Inkjet printing - the physics of manipulating liquid jets and drops.* Engineering and Physics - Synergy for Success, 2008. **105**.
61. Derby, B., *Inkjet Printing of Functional and Structural Materials: Fluid Property Requirements, Feature Stability, and Resolution.* Annual Review of Materials Research, Vol 40, 2010. **40**: p. 395-414.
62. Reis, N., C. Ainsley, and B. Derby, *Ink-jet delivery of particle suspensions by piezoelectric droplet ejectors.* Journal of Applied Physics, 2005. **97**(9).
63. Dijksman, J.F., D.B. van Dam, P.C. Duineveld, and J.E. Rubingh, *Precision inkjet printing of polymer light emitting diode displays.* DPP 2005: International Conference on Digital Production Printing and Industrial Applications, Final Program and Proceedings, 2005: p. 133.
64. Wijshoff, H., *The dynamics of the piezo inkjet printhead operation.* Physics Reports-Review Section of Physics Letters, 2010. **491**(4-5): p. 77-177.
65. Bogy, D.B. and F.E. Talke, *Experimental and Theoretical-Study of Wave-Propagation Phenomena in Drop-on-Demand Ink Jet Devices.* Ibm Journal of Research and Development, 1984. **28**(3): p. 314-321.
66. Tekin, E., P.J. Smith, and U.S. Schubert, *Inkjet printing as a deposition and patterning tool for polymers and inorganic particles.* Soft Matter, 2008. **4**(4): p. 703-713.
67. Hoth, C.N., S.A. Choulis, P. Schilinsky, and C.J. Brabec, *High photovoltaic performance of inkjet printed polymer: Fullerene blends.* Advanced Materials, 2007. **19**(22): p. 3973-78.

68. Stokes, G., *On the theories of the internal friction in fluids in motion, and of the equilibrium and motion of elastic solids.* Transaction of the Cambridge Philosophical Society, 1845. **8**(22): p. 287-342.
69. Derby, B. and N. Reis, *Inkjet printing of highly loaded particulate suspensions.* Mrs Bulletin, 2003. **28**(11): p. 815-818.
70. Dijksman, J.F., *Hydrodynamics of Small Tubular Pumps.* Journal of Fluid Mechanics, 1984. **139**(Feb): p. 173-191.
71. Yunker, P.J., T. Still, M.A. Lohr, and A.G. Yodh, *Suppression of the coffee-ring effect by shape-dependent capillary interactions.* Nature, 2011. **476**(7360): p. 308-11.
72. Fu, S.H., G.F. Zhang, C.S. Du, and A.L. Tian, *Preparation of Encapsulated Disperse Dye Dispersion for Polyester Inkjet Printing Ink.* Journal of Applied Polymer Science, 2011. **121**(3): p. 1616-1621.
73. Takeichi, M., *Cadherin Cell-Adhesion Receptors as a Morphogenetic Regulator.* Science, 1991. **251**(5000): p. 1451-1455.
74. Hynes, R.O., *Integrins: versatility, modulation, and signaling in cell adhesion.* Cell, 1992. **69**(1): p. 11-25.
75. Boterberg, T., M.E. Bracke, E.A. Bruyneel, and M.M. Mareel, *Cell aggregation assays.* Methods Mol Med, 2001. **58**: p. 33-45.
76. Kim, S.H., Z. Li, and D.B. Sacks, *E-cadherin-mediated cell-cell attachment activates Cdc42.* J Biol Chem, 2000. **275**(47): p. 36999-7005.
77. Hur, S.C., N.K. Henderson-MacLennan, E.R.B. McCabe, and D. Di Carlo, *Deformability-based cell classification and enrichment using inertial microfluidics.* Lab on a Chip, 2011. **11**(5): p. 912-920.
78. Mustin, B. and B. Stoeber, *Deposition of particles from polydisperse suspensions in microfluidic systems.* Microfluidics and Nanofluidics, 2010. **9**(4-5): p. 905-913.
79. Guha, A., *Transport and deposition of particles in turbulent and laminar flow.* Annual Review of Fluid Mechanics, 2008. **40**: p. 311-341.
80. Stamm, M.T., T. Gudipaty, C. Rush, L.N. Jiang, and Y. Zohar, *Particle aggregation rate in a microchannel due to a dilute suspension flow.* Microfluidics and Nanofluidics, 2011. **11**(4): p. 395-403.
81. Park, J., S. Chung, H. Yun, K.C. Cho, C.A. Chung, D.C. Han, and J.K. Chang, *Asymmetric nozzle structure for particles converging into a highly confined region.* Current Applied Physics, 2006. **6**(6): p. 992-995.
82. Parsa, S., M. Gupta, F. Loizeau, and K.C. Cheung, *Effects of surfactant and gentle agitation on inkjet dispensing of living cells.* Biofabrication, 2010. **2**(2).
83. Sirringhaus, H. and T. Shimoda, *Inkjet printing of functional materials.* Mrs Bulletin, 2003. **28**(11): p. 802-803.
84. Lee, H.H., K.S. Chou, and K.C. Huang, *Inkjet printing of nanosized silver colloids.* Nanotechnology, 2005. **16**(10): p. 2436-2441.
85. Li, B., P.W. Ryan, B.H. Ray, K.J. Leister, N.M.S. Sirimuthu, and A.G. Ryder, *Rapid Characterization and Quality Control of Complex Cell Culture Media Solutions Using Raman Spectroscopy and Chemometrics.* Biotechnology and Bioengineering, 2010. **107**(2): p. 290-301.
86. Olea, N., M. Villalobos, J.M.R. Dealmodovar, and V. Pedraza, *Mcf-7 Breast-Cancer Cells Grown as Multicellular Spheroids Invitro - Effect of 17-Beta-Estradiol.* International Journal of Cancer, 1992. **50**(1): p. 112-117.

87. English, D. and B.R. Andersen, *Single-step separation of red blood cells. Granulocytes and mononuclear leukocytes on discontinuous density gradients of Ficoll-Hypaque.* J Immunol Methods, 1974. **5**(3): p. 249-52.
88. Healthcare, G., *Ficoll PM 70, Ficoll PM 400*.
89. Pandit, N., T. Trygstad, S. Croy, M. Bohorquez, and C. Koch, *Effect of Salts on the Micellization, Clouding, and Solubilization Behavior of Pluronic F127 Solutions.* J Colloid Interface Sci, 2000. **222**(2): p. 213-220.
90. Parsa, S., M. Gupta, F. Loizeau, and K.C. Cheung, *Effects of surfactant and gentle agitation on inkjet dispensing of living cells.* Biofabrication, 2010. **2**(2): p. 025003.
91. Burg, T.P., M. Godin, S.M. Knudsen, W. Shen, G. Carlson, J.S. Foster, K. Babcock, and S.R. Manalis, *Weighing of biomolecules, single cells and single nanoparticles in fluid.* Nature, 2007. **446**(7139): p. 1066-9.
92. Griwatz, C., B. Brandt, G. Assmann, and K.S. Zanker, *An immunological enrichment method for epithelial cells from peripheral blood.* J Immunol Methods, 1995. **183**(2): p. 251-65.
93. Bryan, A.K., A. Goranov, A. Amon, and S.R. Manalis, *Measurement of mass, density, and volume during the cell cycle of yeast.* Proc Natl Acad Sci U S A, 2010. **107**(3): p. 999-1004.
94. Chahal, D., A. Ahmadi, and K.C. Cheung, *Improving piezoelectric cell printing accuracy and reliability through neutral buoyancy of suspensions.* Biotechnol Bioeng, 2012.
95. Stockert, J.C., A. Blazquez-Castro, M. Canete, R.W. Horobin, and A. Villanueva, *MTT assay for cell viability: Intracellular localization of the formazan product is in lipid droplets.* Acta Histochem, 2012.
96. Yamazoe, H. and T. Tanabe, *Cell micropatterning on an albumin-based substrate using an inkjet printing technique.* Journal of Biomedical Materials Research Part A, 2009. **91A**(4): p. 1202-09.
97. Wang, W., Y. Huang, M. Grujicic, and D.B. Chrisey, *Study of impact-induced mechanical effects in cell direct writing using smooth particle hydrodynamic method.* Journal of Manufacturing Science and Engineering-Transactions of the Asme, 2008. **130**(2).
98. Nair, K., M. Gandhi, S. Khalil, K.C. Yan, M. Marcolongo, K. Barbee, and W. Sun, *Characterization of cell viability during bioprinting processes.* Biotechnol J, 2009. **4**(8): p. 1168-77.
99. Xu, T., J. Jin, C. Gregory, J.J. Hickman, and T. Boland, *Inkjet printing of viable mammalian cells.* Biomaterials, 2005. **26**(1): p. 93-9.
100. Wang, X., W.W. Carr, D.G. Bucknall, and J.F. Morris, *High-shear-rate capillary viscometer for inkjet inks.* Review of Scientific Instruments, 2010. **81**(6).
101. Reis, N., C. Ainsley, and B. Derby, *Viscosity and acoustic behavior of ceramic suspensions optimized for phase-change ink-jet printing.* Journal of the American Ceramic Society, 2005. **88**(4): p. 802-8.
102. Pipe, C.J., T.S. Majmudar, and G.H. McKinley, *High shear rate viscometry.* Rheologica Acta, 2008. **47**(5-6): p. 621-42.
103. Jeong, S., H.C. Song, W.W. Lee, Y. Choi, and B.H. Ryu, *Preparation of aqueous Ag Ink with long-term dispersion stability and its inkjet printing for fabricating conductive tracks on a polyimide film.* Journal of Applied Physics, 2010. **108**(10).

104. Veerman, E.C., Valentijn-Benz, M., Nieuw Amerongnen, A.V., *Viscosity of human salivary mucins: effect of pH and ionic strength and role of sialic acid.* Journal de Biologique Buccale, 1989. **17**(4): p. 297-306.
105. Stracher, A., *Effect of pH and urea on the optical rotation, viscosity, and adenosinetriphosphatase activity of myosin A.* The Journal of Biological Chemistry, 1961. **236**(9): p. 2467-71.
106. Justice, C., Brix, A., Freimark, D., Kraume, M., Pfromm, P., Eichenmueller, B., Czermak, P., *Process control in cell culture technology using dielectric spectroscopy.* Biotechnology Advances, 2011. **29**(4): p. 391-401.
107. Famili, A., S.A. Palkar, and W.J. Baldy, *First drop dissimilarity in drop-on-demand inkjet devices.* Physics of Fluids, 2011. **23**(1).
108. Inglis, D.W., R. Riehn, R.H. Austin, and J.C. Sturm, *Continuous microfluidic immunomagnetic cell separation.* Applied Physics Letters, 2004. **85**(21): p. 5093-95.
109. Kepkay, P.E., *Particle Aggregation and the Biological Reactivity of Colloids.* Marine Ecology-Progress Series, 1994. **109**(2-3): p. 293-304.
110. Hang, H.F., Y.X. Guo, J. Liu, L. Bai, J.Y. Xia, M.J. Guo, and M. Hui, *Computational Fluid Dynamics Modeling of an Inverted Frusto-conical Shaking Bioreactor for Mammalian Cell Suspension Culture.* Biotechnology and Bioprocess Engineering, 2011. **16**(3): p. 567-75.
111. Wang, G.R., N.M. Qi, and Z.M. Wang, *Application of a stir-tank bioreactor for perfusion culture and continuous harvest of Glycyrrhiza inflata suspension cells.* African Journal of Biotechnology, 2010. **9**(3): p. 347-51.
112. Collignon, M.L., D. Dossin, A. Delafosse, M. Crine, and D. Toye, *Quality of mixing in a stirred bioreactor used for animal cells culture: heterogeneities in a lab scale bioreactor and evolution of mixing time with scale up.* Biotechnologie Agronomie Societe Et Environnement, 2010. **14**: p. 585-91.
113. Wang, Z.W. and J.M. Belovich, *A Simple Apparatus for Measuring Cell Settling Velocity.* Biotechnology Progress, 2010. **26**(5): p. 1361-66.
114. Crocker, J.C. and D.G. Grier, *Methods of digital video microscopy for colloidal studies.* Journal of Colloid and Interface Science, 1996. **179**(1): p. 298-310.
115. *CyQUANT NF Cell Proliferation Assay Kit*, Invitrogen, Editor. 2006.
116. Boutard, N., S. Turcotte, K. Beauregard, C. Quiniou, S. Chemtob, and W.D. Lubell, *Examination of the active secondary structure of the peptide 101.10, an allosteric modulator of the interleukin-1 receptor, by positional scanning using beta-amino gamma-lactams.* Journal of Peptide Science, 2011. **17**(4): p. 288-96.
117. Launiere, C.A., G.J. Czaplewski, J.H. Myung, S. Hong, and D.T. Eddington, *Rheologically biomimetic cell suspensions for decreased cell settling in microfluidic devices.* Biomedical Microdevices, 2011. **13**(3): p. 549-57.
118. Munson, M.S., J.M. Spotts, A. Niemisto, J. Selinummi, J.G. Kralj, M.L. Salit, and A. Ozinsky, *Image-based feedback control for real-time sorting of microspheres in a microfluidic device.* Lab Chip, 2010. **10**(18): p. 2402-10.
119. Alon, R. and K. Ley, *Cells on the run: shear-regulated integrin activation in leukocyte rolling and arrest on endothelial cells.* Current Opinion in Cell Biology, 2008. **20**(5): p. 525-32.
120. Shi, Z.D. and J.M. Tarbell, *Fluid flow mechanotransduction in vascular smooth muscle cells and fibroblasts.* Ann Biomed Eng, 2011. **39**(6): p. 1608-19.

121. Gaehtgens, P., C. Duhrssen, and K.H. Albrecht, *Motion, Deformation, and Interaction of Blood-Cells and Plasma during Flow through Narrow Capillary Tubes.* Blood Cells, 1980. **6**(4): p. 799-812.
122. McEver, R.P. and C. Zhu, *Rolling Cell Adhesion.* Annual Review of Cell and Developmental Biology, Vol 26, 2010. **26**: p. 363-96.
123. Shin, S., M.S. Park, Y.H. Ku, and J.S. Suh, *Shear-dependent aggregation characteristics of red blood cells in a pressure-driven microfluidic channel.* Clin Hemorheol Microcirc, 2006. **34**(1-2): p. 353-61.
124. Leighton, D. and A. Acrivos, *Viscous Resuspension.* Chemical Engineering Science, 1986. **41**(6): p. 1377-84.
125. Lebedev-Stepanov, P.V. and O.V. Rudenko, *Sound attenuation in a liquid containing suspended particles of micron and nanometer dimensions.* Acoustical Physics, 2009. **55**(6): p. 729-34.
126. de Gans, B.J. and U.S. Schubert, *Inkjet printing of well-defined polymer dots and arrays.* Langmuir, 2004. **20**(18): p. 7789-93.
127. Taylor, D.L.a.G., K.A., *Multiplexed high content screening assays create a systems cell biology approach to drug discovery.* Drug Discov Today: Technologies, 2005. **2**(2): p. 149 - 54.
128. Butcher, E.C., E.L. Berg, and E.J. Kunkel, *Systems biology in drug discovery.* Nat Biotechnol, 2004. **22**(10): p. 1253-9.
129. Friedl, P. and J.A. Zallen, *Dynamics of cell-cell and cell-matrix interactions in morphogenesis, regeneration and cancer.* Current Opinion in Cell Biology, 2010. **22**(5): p. 557-9.
130. Calvert, P., *Materials science. Printing cells.* Science, 2007. **318**(5848): p. 208-9.